

SWD and seismic interferometry

Flavio Poletto *

(*) OGS (Istituto Nazionale di Oceanografia e Geofisica Sperimentale)
Trieste- ITALY

Email: fpoletto@ogs.trieste.it

**XIV GIAMBIAGI
WINTER SCHOOL**
Applied and Environmental Geophysics
July 16 to 20, 2012

Outline



- ☐ SWD concept
- ☐ SWD using the working drill-bit as a source
- ☐ Examples

- ☐ Introduction to seismic interferometry (SI)
- ☐ Concepts and applications
- ☐ Multidimensional wavefield representation

Part 1 - Seismic while drilling (SWD)



- ❑ SWD concept
- ❑ SWD using the working drill-bit as a source
- ❑ Examples

- ❑ Introduction to seismic interferometry (SI)
- ❑ Concepts and applications
- ❑ Multidimensional wavefield representation

Motivation for SWD

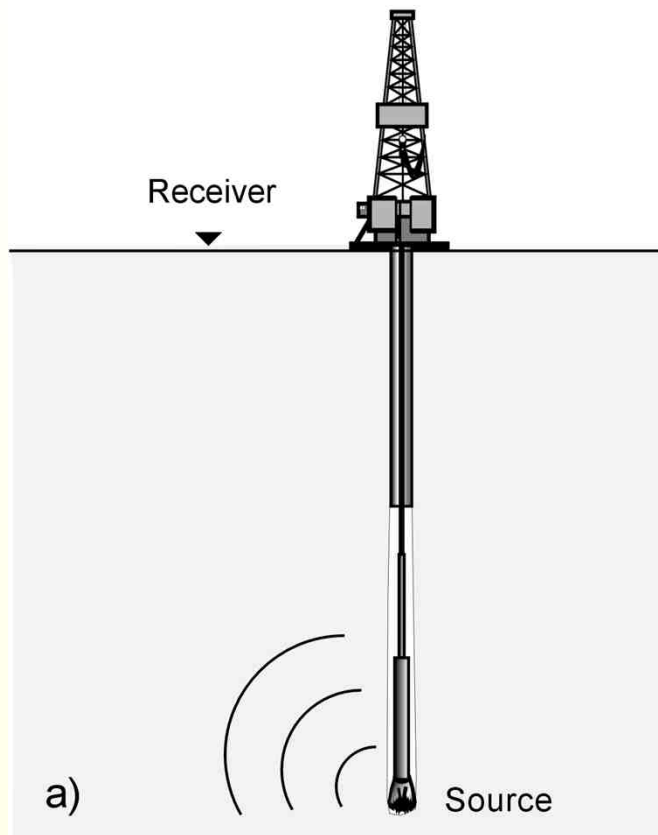


- ❑ Provides geophysical information while drilling a well, in relevant time to take drilling decisions
- ❑ Updates WD the geophysical model based on pre-drilling data (exploration)
- ❑ Continuously available, predicts the interfaces and calibrates the time-depth sections WD and logs
- ❑ Reduces the risk, no drill pipes out of the hole
- ❑ Reduces costs, no need to interrupt drilling and stand by
- ❑ Usable where conventional methods are not applicable

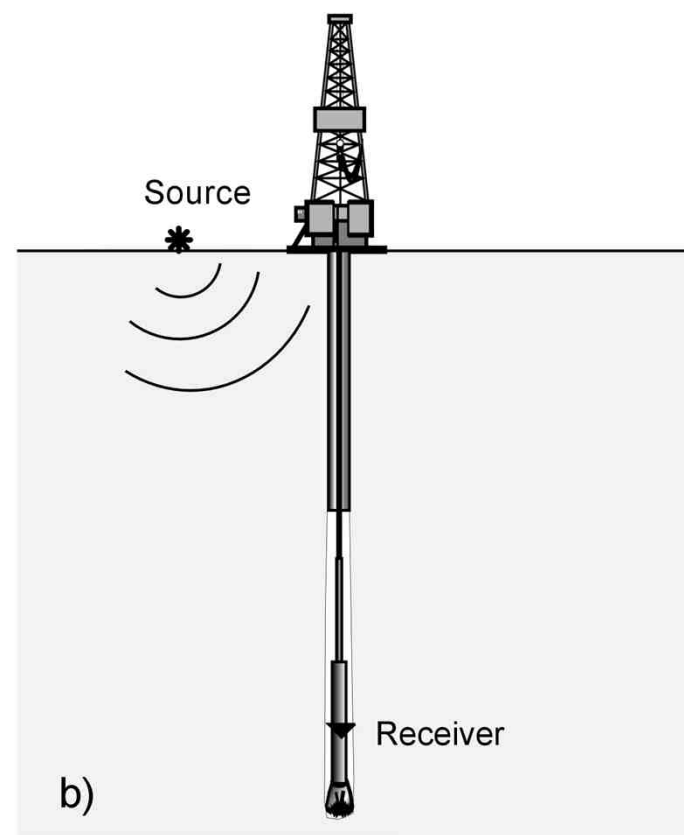
Normal and reverse WD VSP geometry



RECIPROCAL (REVERSE) VSP



NORMAL VSP

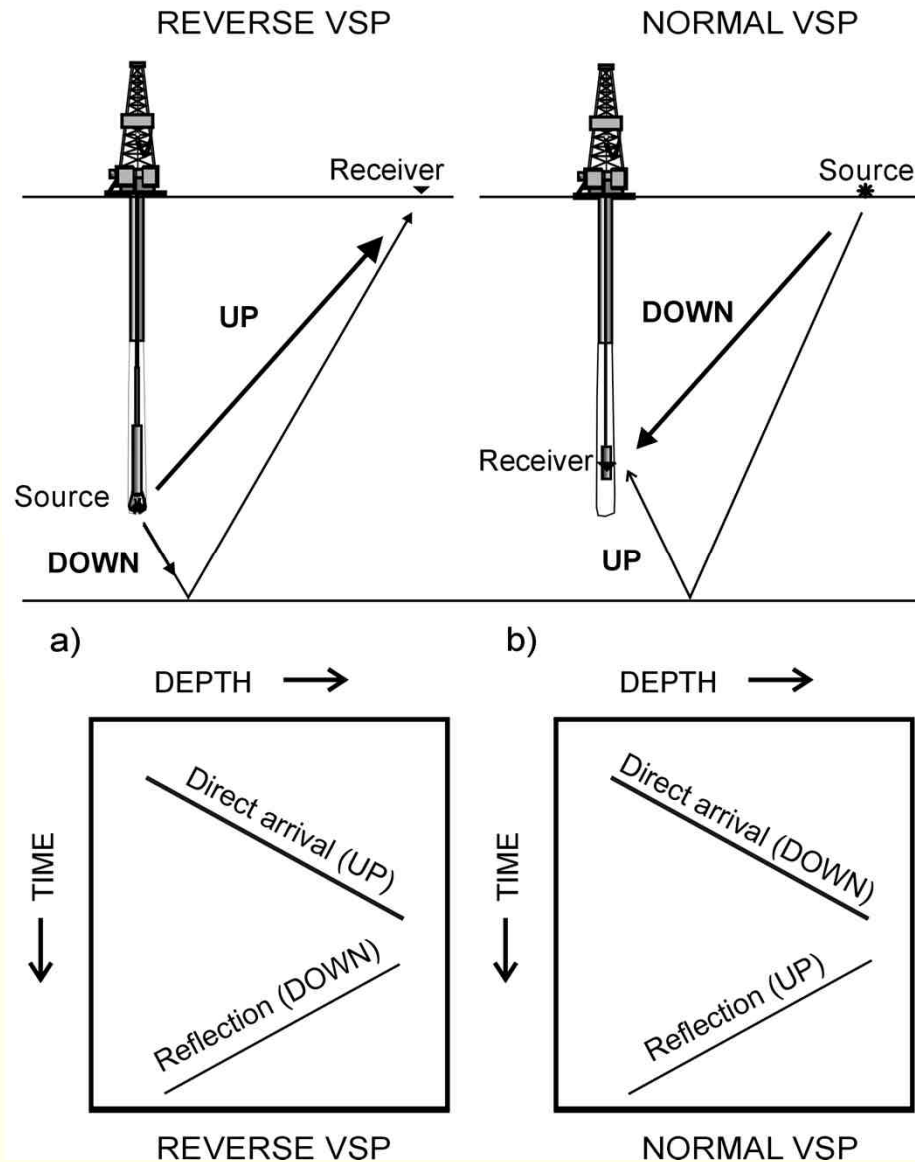


(After Poletto and Miranda, 2004)

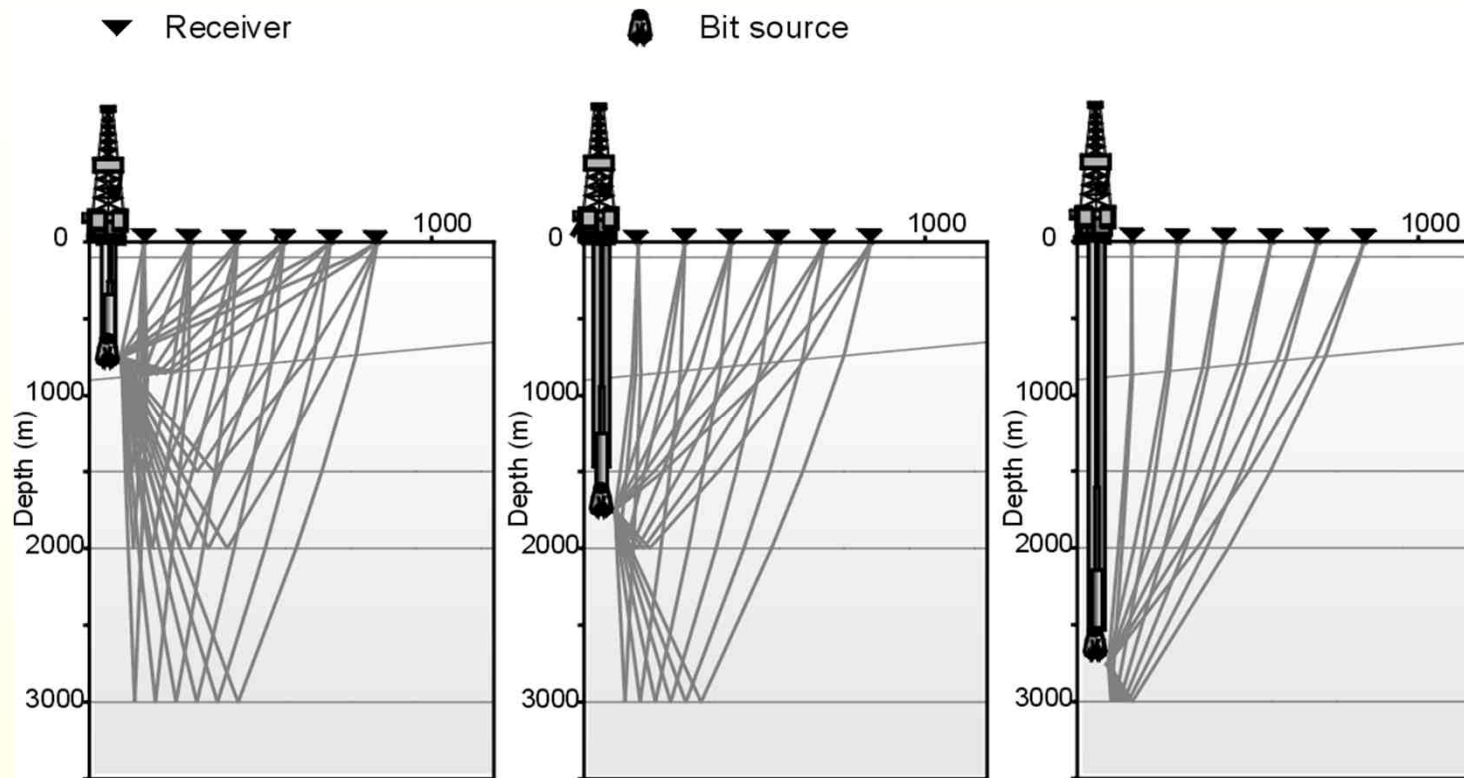
VSP wavefields



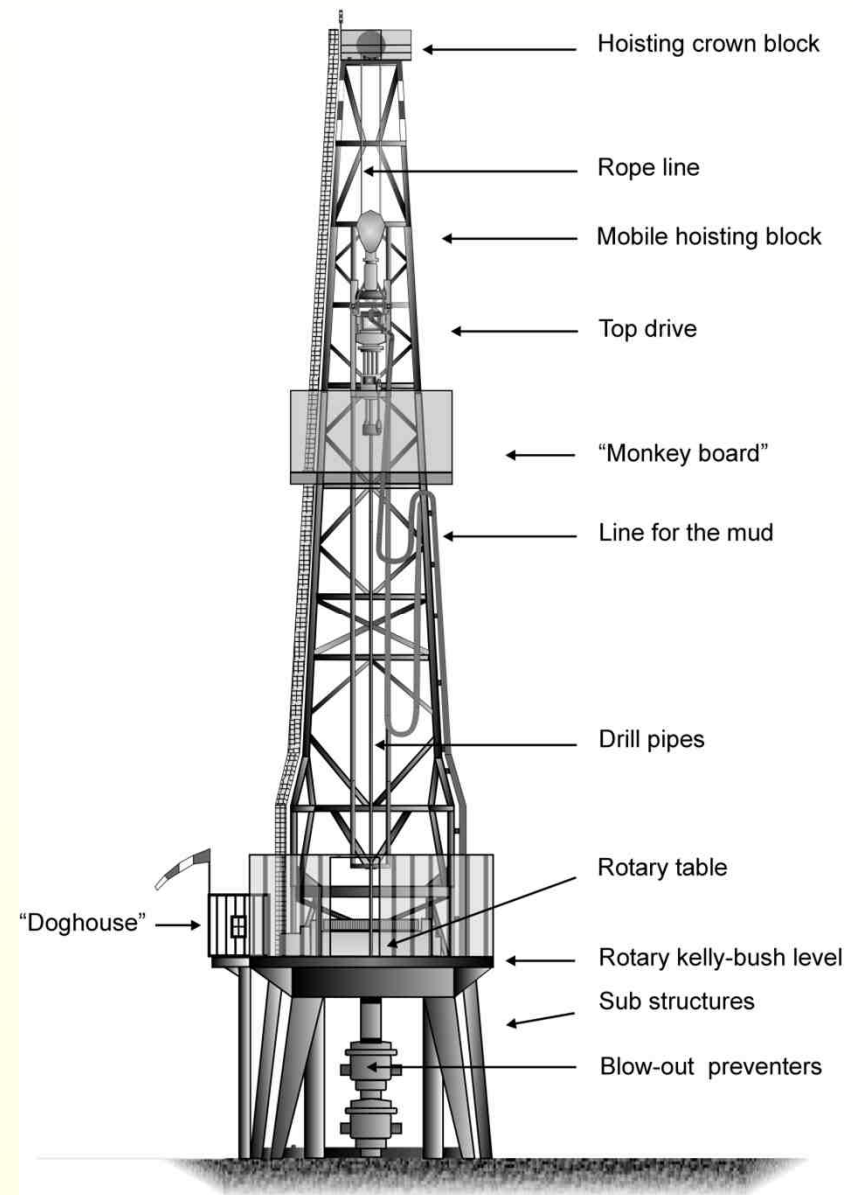
WAVEFIELDS IN REVERSE AND NORMAL VSP



WD RVSP wavefields



Derrick system



Working Drill-bit as a SWD vibration source

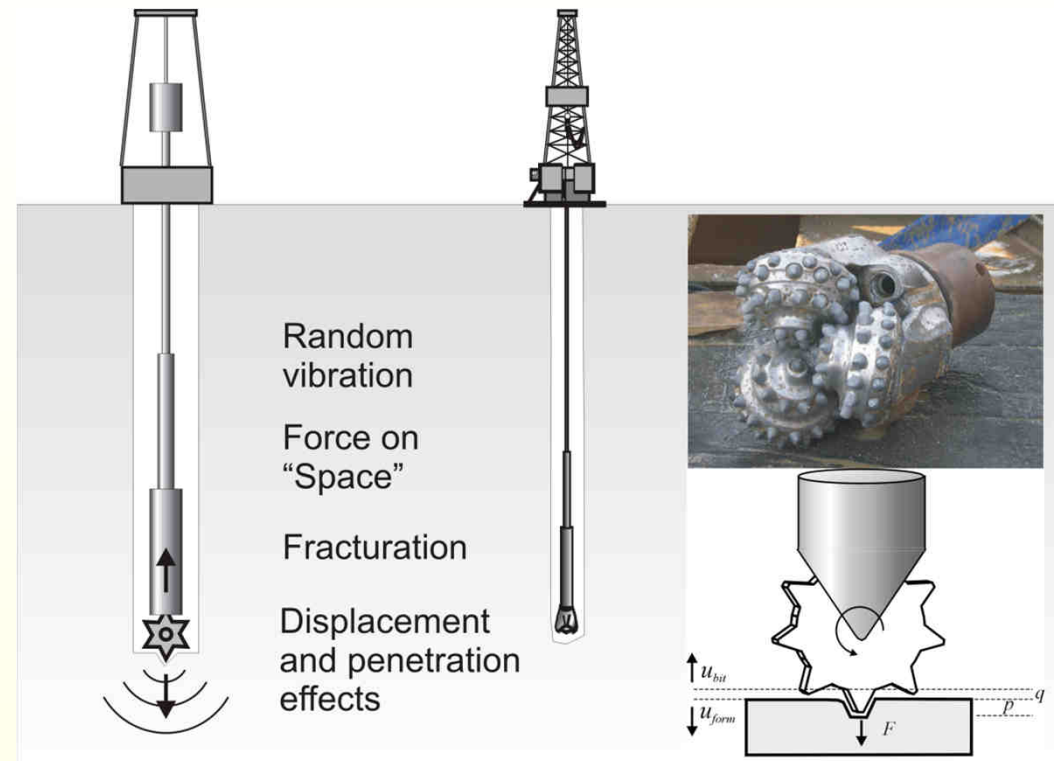


The concept is to use the vibrations produced by a working drilling bit as a seismic signal.

Detail of roller-cone bit source



Working Drill-bit as a SWD vibration source



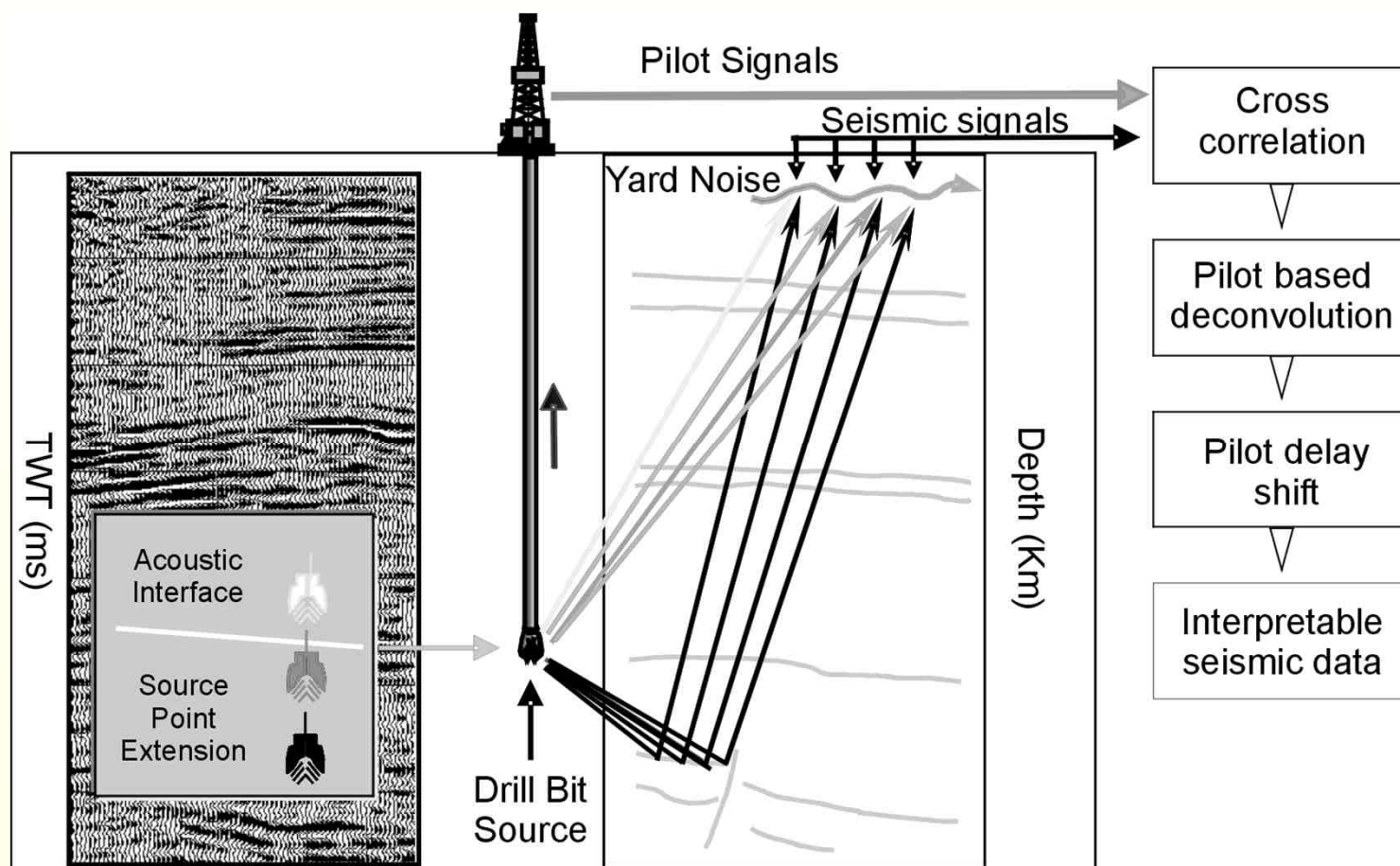
Source performance depends on drilling conditions and formation properties

Drill-bit SWD method



Surface recording line deployed
in the proximity of the well

Drill-bit SWD processing method



(After Poletto and Miranda, 2004)

Drill-bit SWD processing method



Recall basic concepts in signal correlation

In time

$$c_{BA}(\tau) = \int s_B(t) s_A(\tau + t) dt$$

Convolution with reversal

$$c_{BA}(\tau) = s_B(t) * s_A(-t)$$

In frequency

$$C_{BA}(\omega) = S_B(\omega) S_A(\omega)^*$$

$$C_{BA}(\omega) = |S_B(\omega)| |S_A(\omega)| e^{i(\phi_B - \phi_A)}$$

Deconvolution (inverse filtering)

$$D_{BA}(\omega) = \frac{|S_B(\omega)|}{|S_A(\omega)|} e^{i(\phi_B - \phi_A)}$$

Drill-bit SWD processing method



Recall basic concepts in signal correlation

In time

$$c_{BA}(\tau) = \int s_B(t) s_A(\tau + t) dt$$

Convolution with reversal

$$c_{BA}(\tau) = s_B(t) * s_A(-t)$$

In frequency

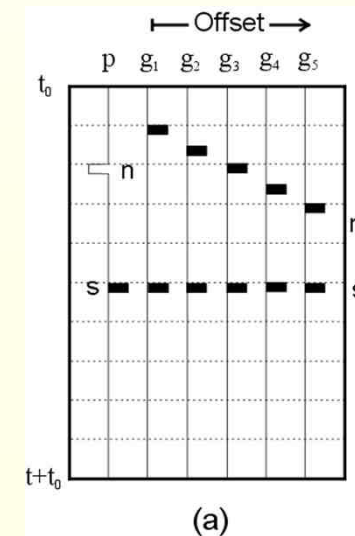
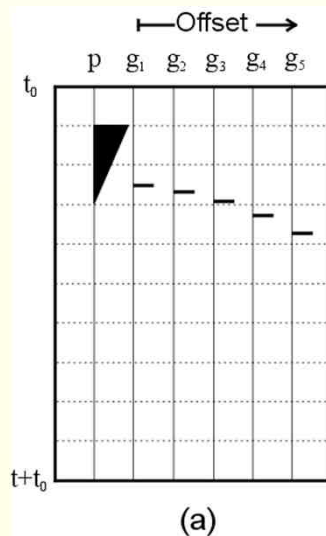
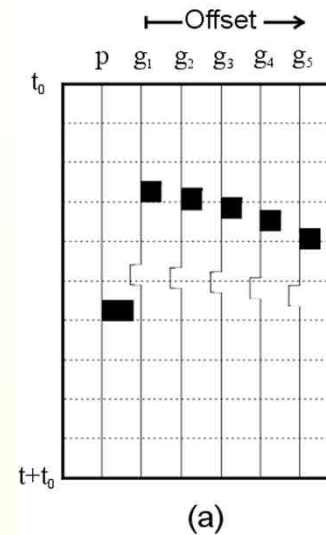
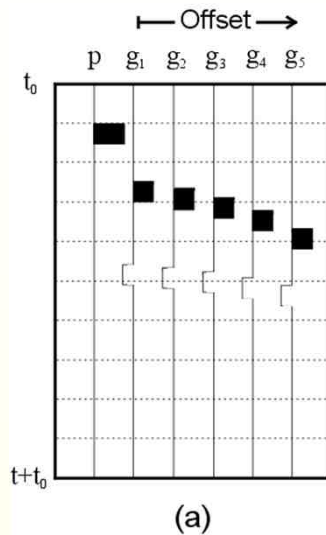
$$C_{BA}(\omega) = S_B(\omega) S_A(\omega)^*$$

$$[C_{BA}(\omega)]^* = C_{AB}(\omega) = S_A(\omega) S_B(\omega)^*$$

Drill-bit SWD processing method



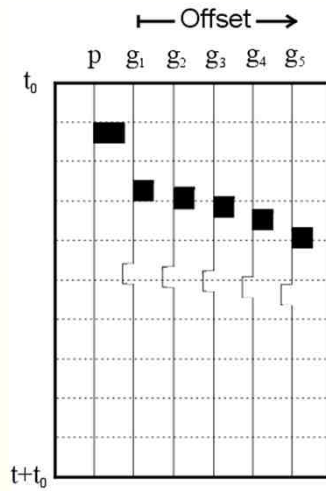
Some basic concepts in signal (a) correlation



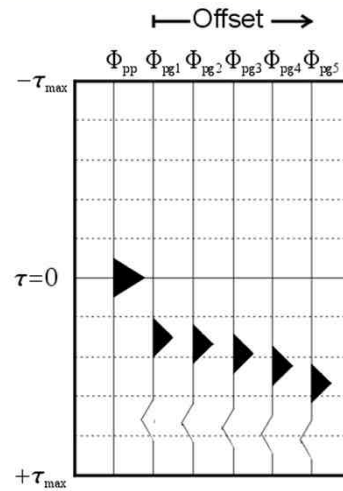
Drill-bit SWD processing method



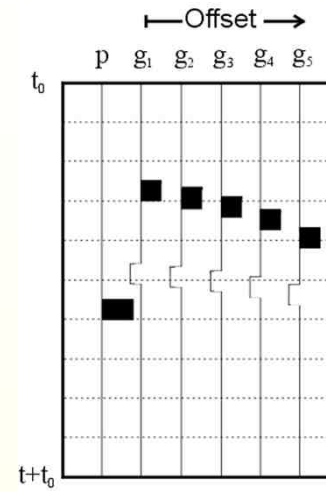
Some basic concepts in signal (a) correlation (b)



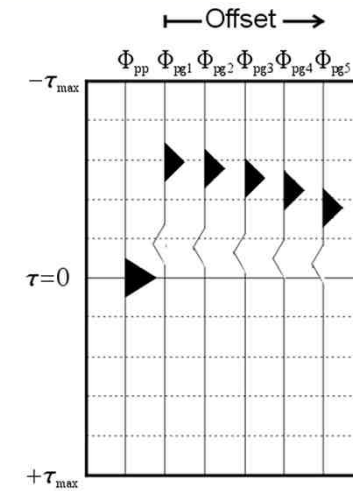
(a)



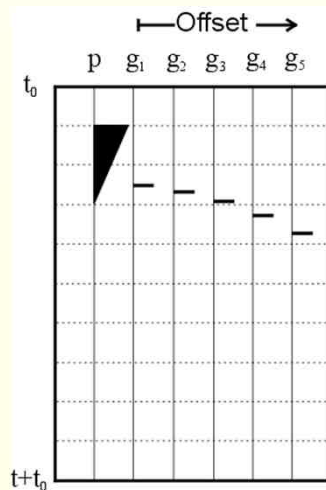
(b)



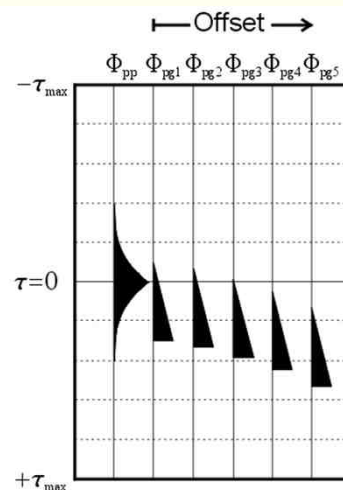
(a)



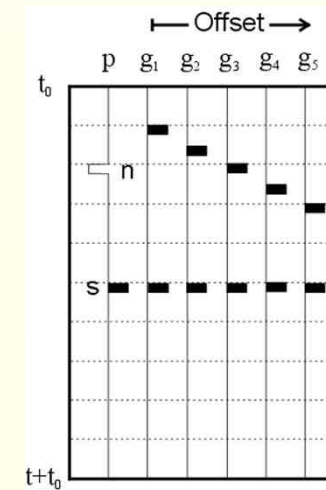
(b)



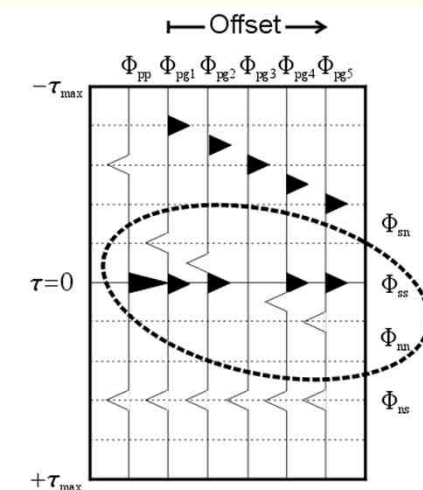
(a)



(b)



(a)

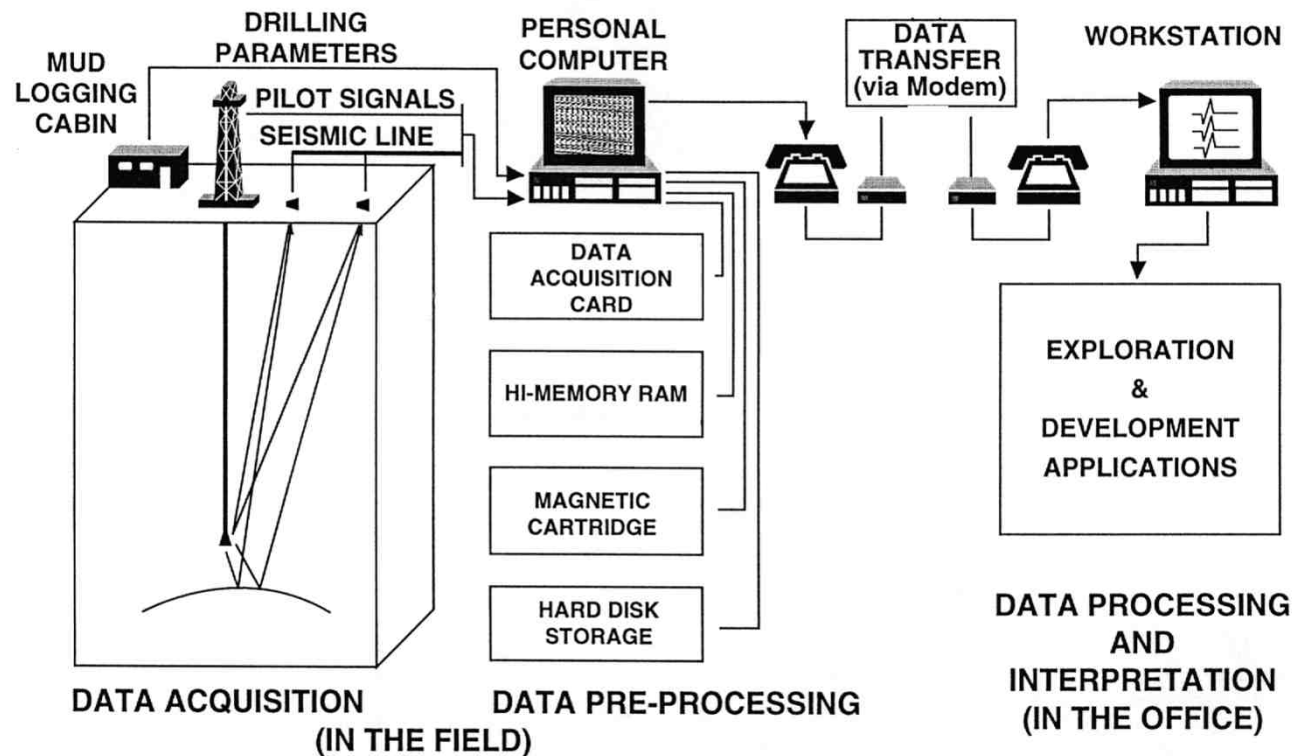


(b)

Drill-bit SWD method

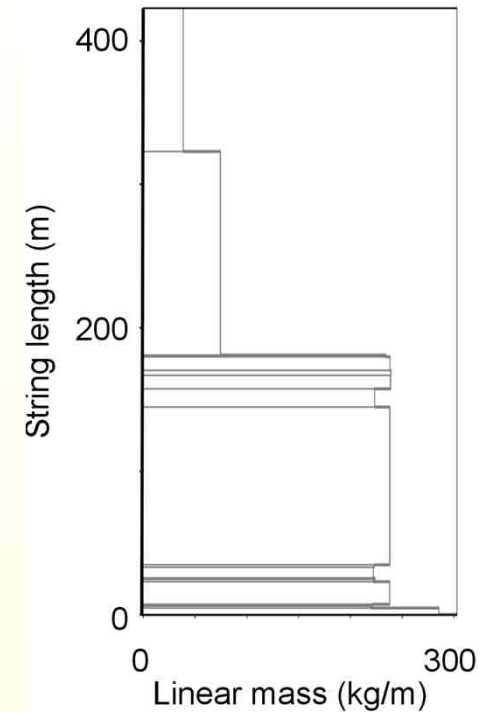
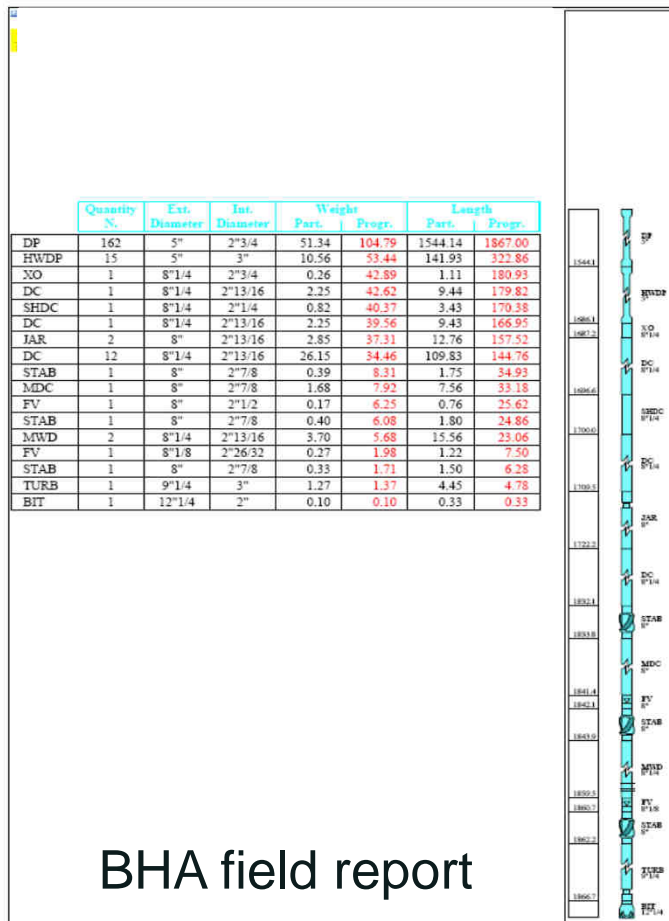


Drill-bit SWD RVSP system



OGS – Eni SEISBIT® Technology

Drill-bit SWD RVSP pilot signal analysis



SEISBIT ® Technology. Uses drill-string info WD

Drill-bit SWD RVSP pilot waves



Thin rod approximation

Velocity

Impedance

Axial

$$V_{ax} = \sqrt{\frac{Y}{\rho}}$$

$$Z_{ax} = A\rho V_{ax}$$

Torsional

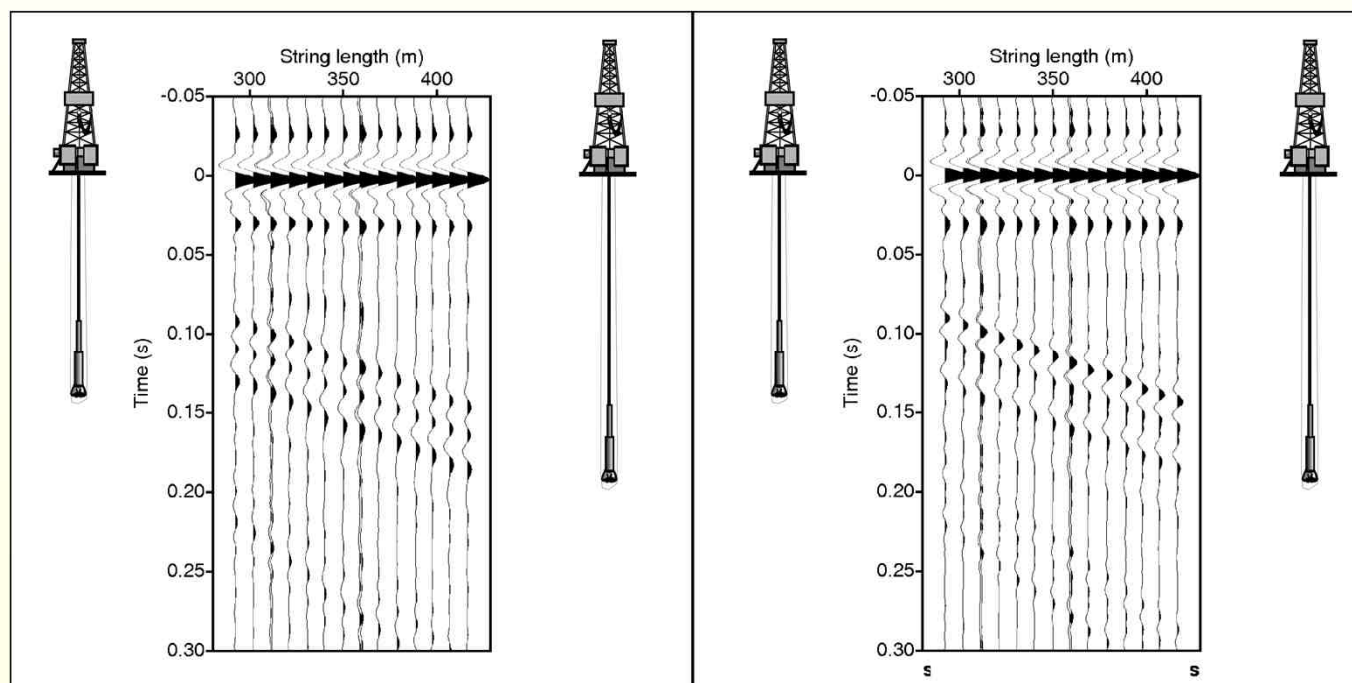
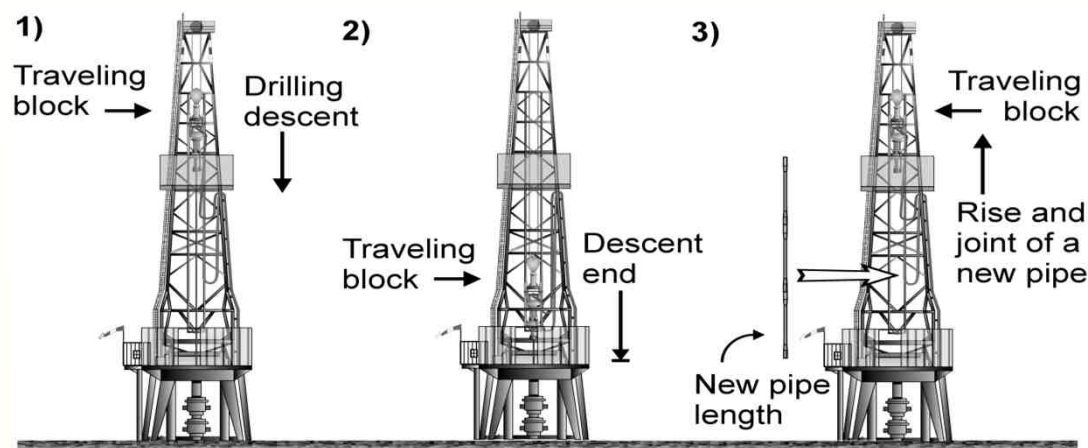
$$V_{tor} = \sqrt{\frac{\mu}{\rho}}$$

$$Z_{tor} = I\rho V_{tor}$$

Reflection coefficient between tubes 1 and 2:

$$c = \frac{Z_2 - Z_1}{Z_2 + Z_1}$$

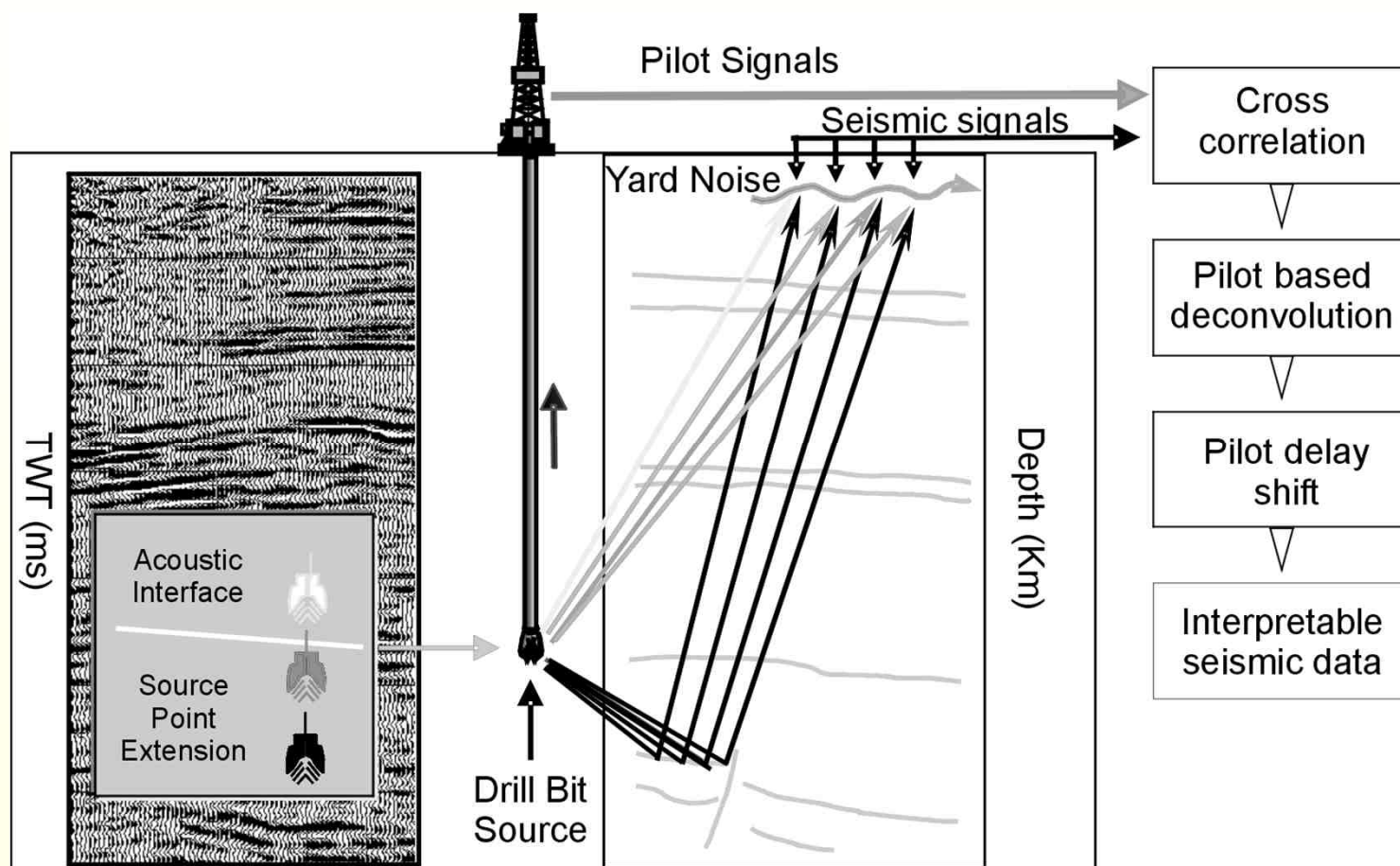
Drill-bit SWD RVSP pilot signal analysis



Real

Synthetic

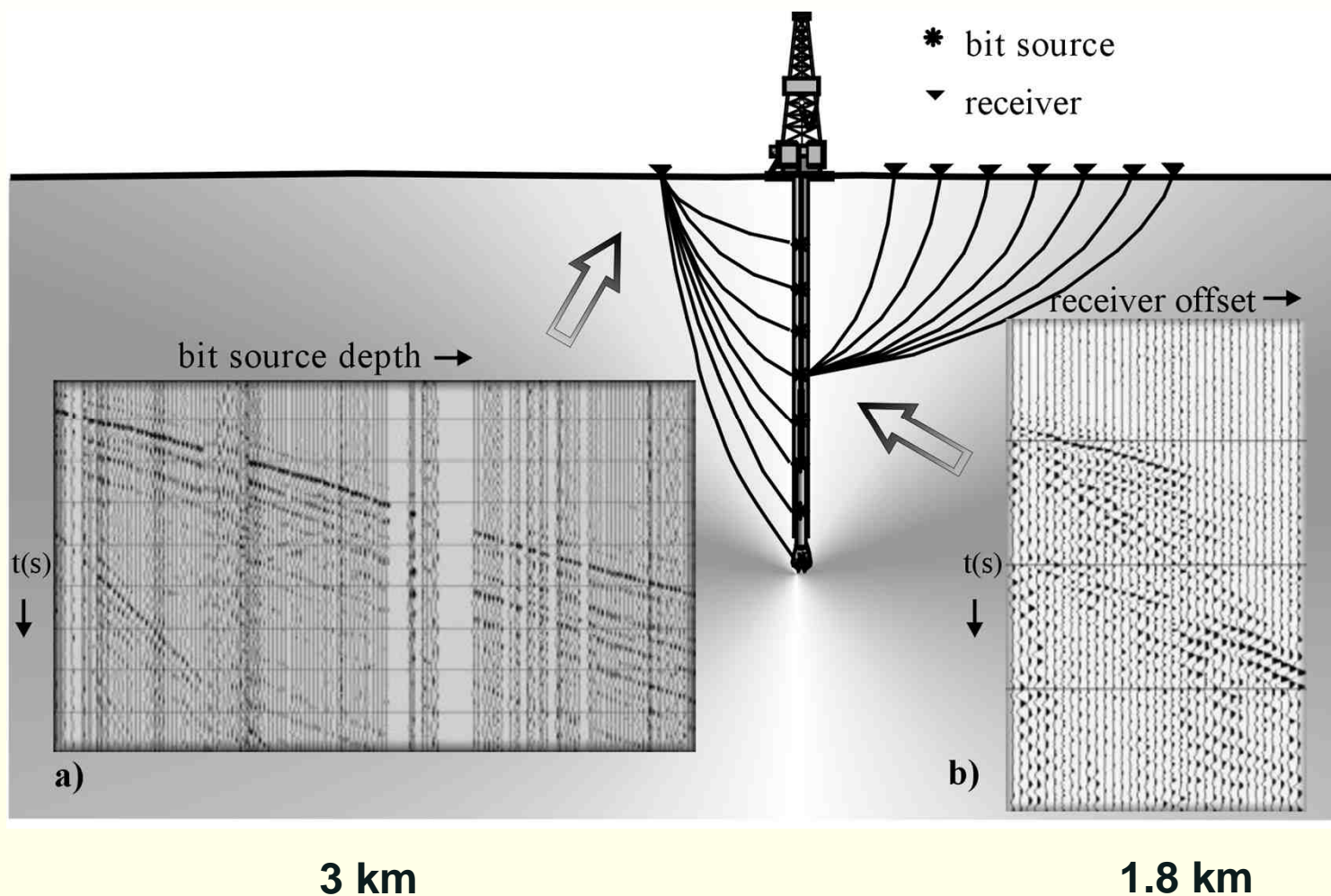
Drill-bit SWD processing method



Drill-bit SWD based on pilot-correlation method



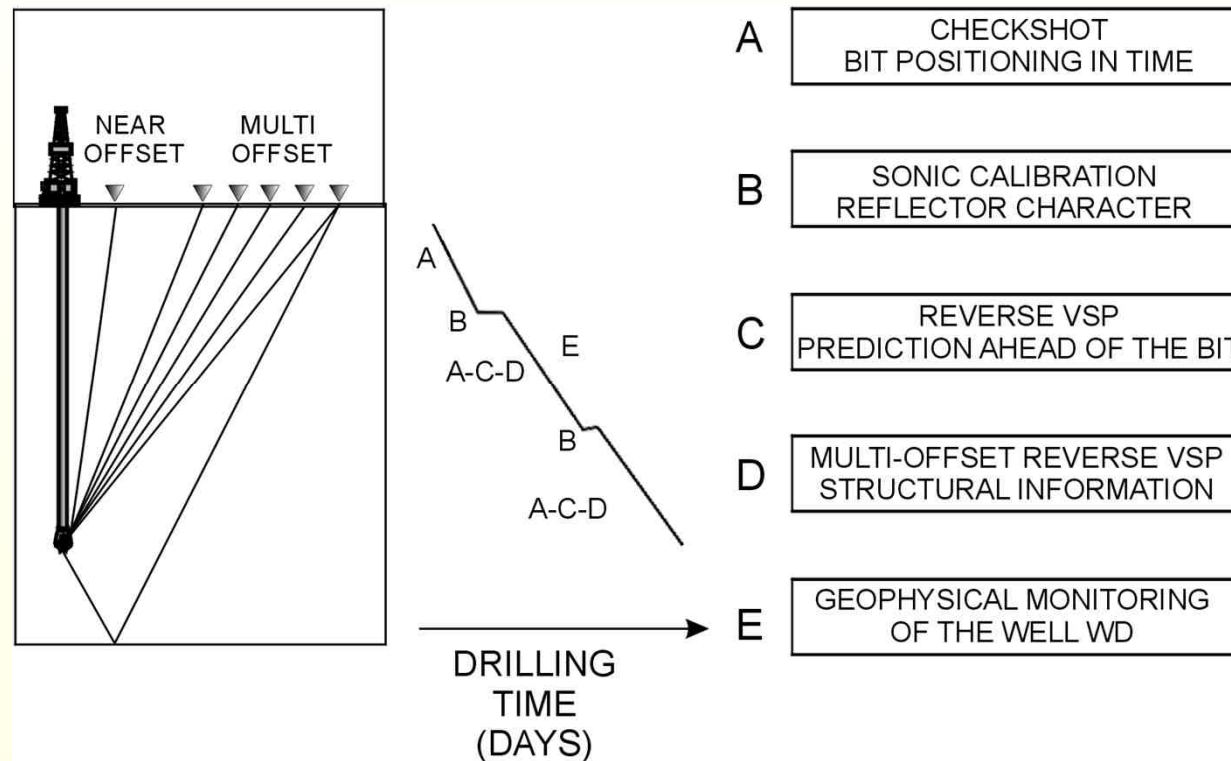
Drill-bit common-receiver and common-source RVSP



Drill-bit SWD based on pilot-correlation method

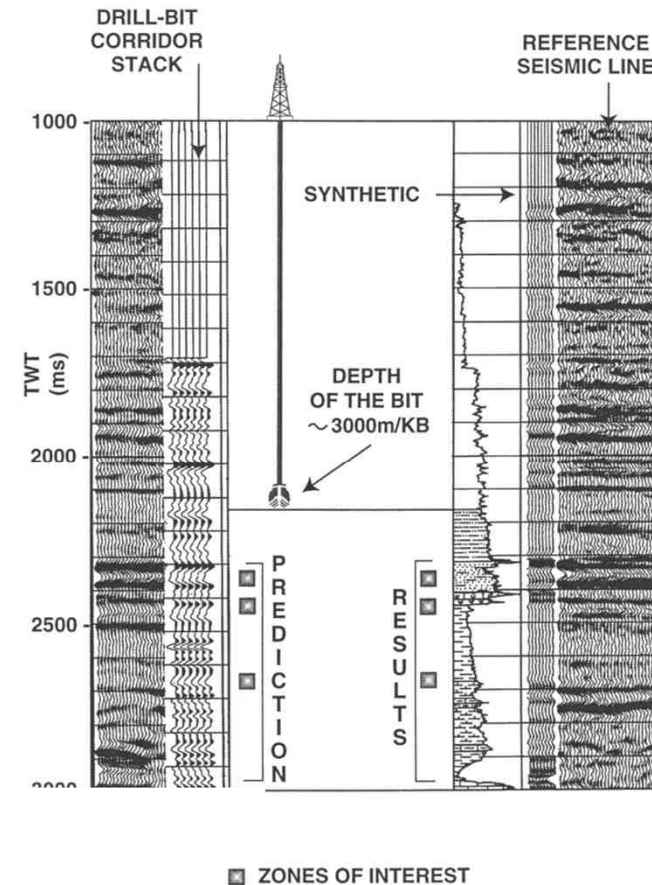
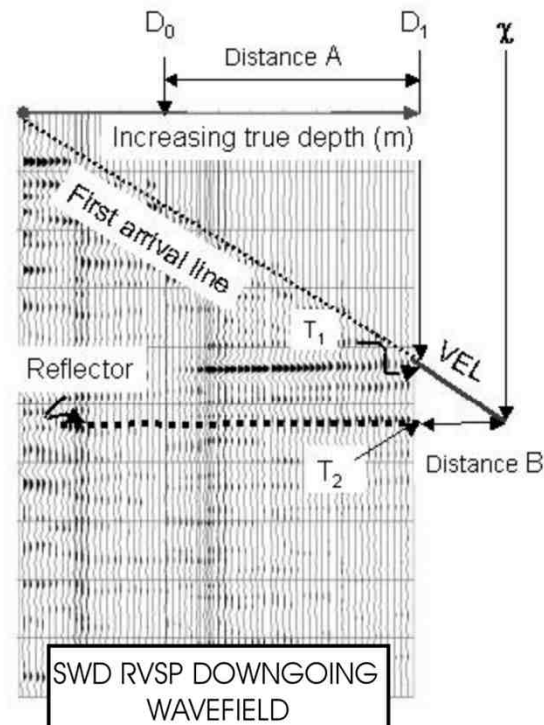


Drill-bit SWD RVSP products



(After Poletto and Miranda, 2004)

Drill-bit SWD based on pilot-correlation method

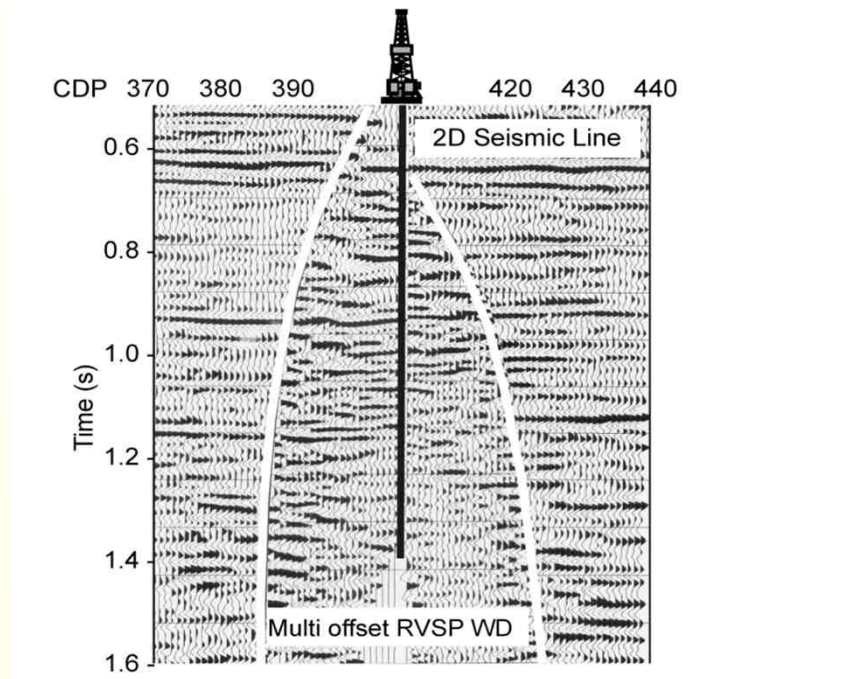


(After Poletto and Miranda, 2004)

Drill-bit SWD based on pilot-correlation method



Drill-bit 2D RVSP maps

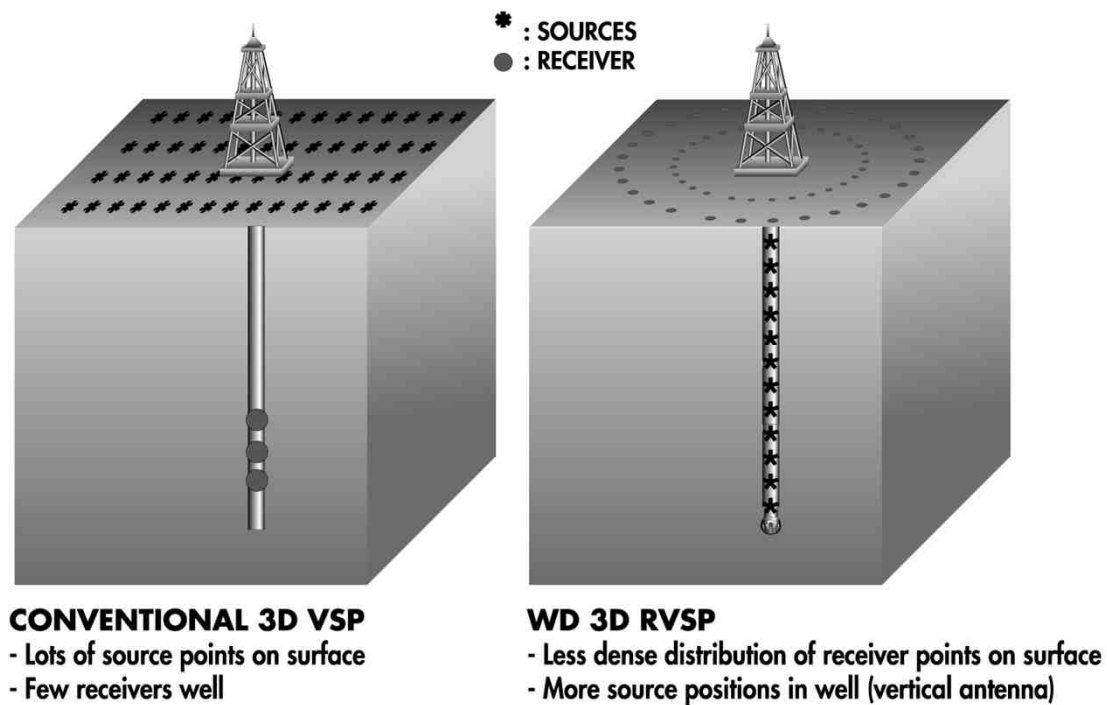


2D multioffset Seismic While Drilling used for prediction ahead of the bit, for structural reconstruction and to update the geophysical model.

3D VSP



ACQUISITION LAYOUT COMPARISON

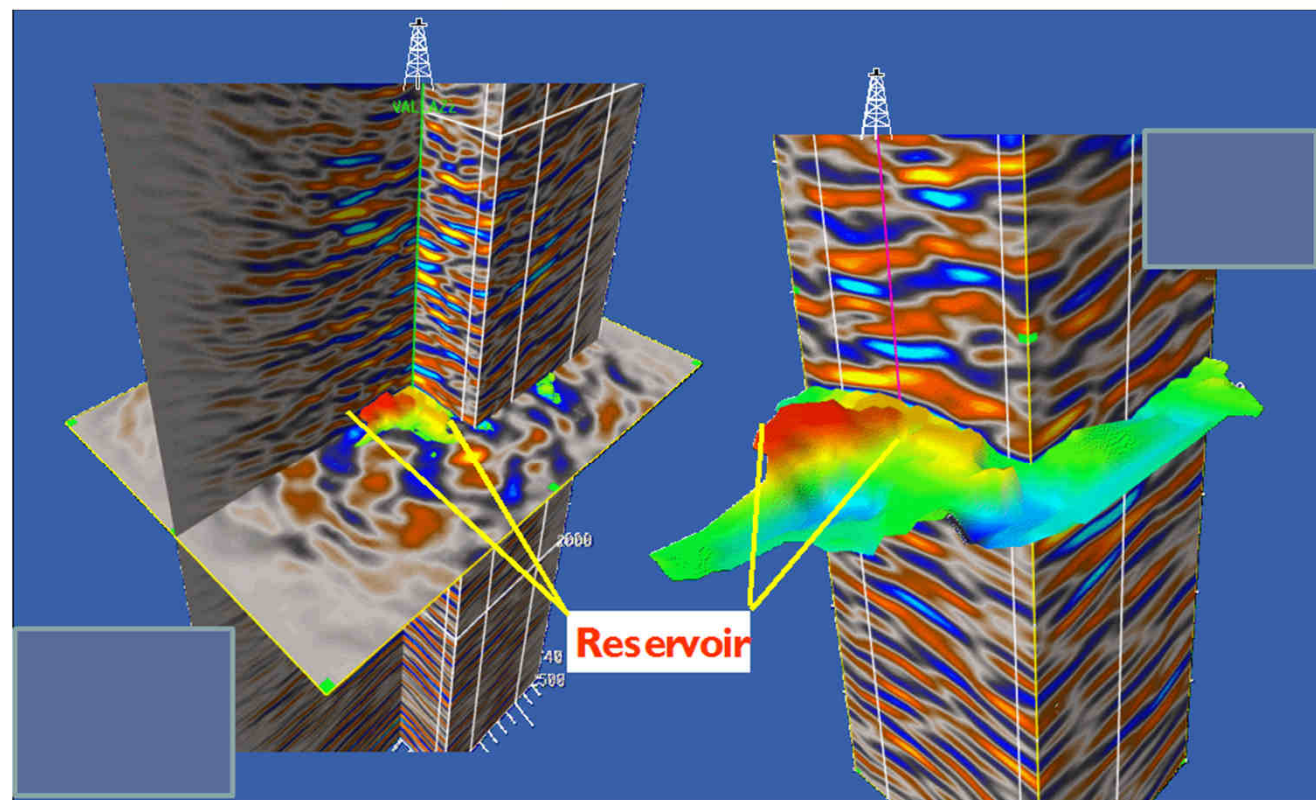
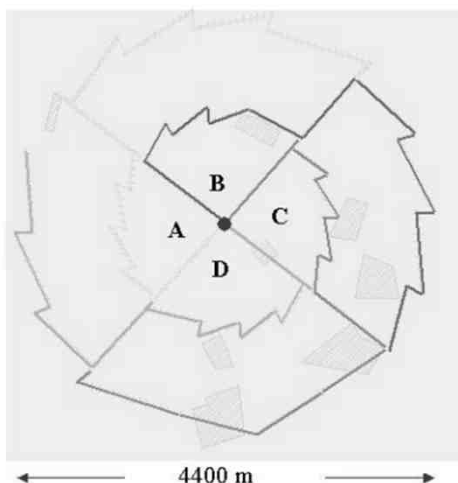


MAIN POINT: OPTIMISATION RECEIVER POSITIONING

Drill-bit SWD based on pilot-correlation method

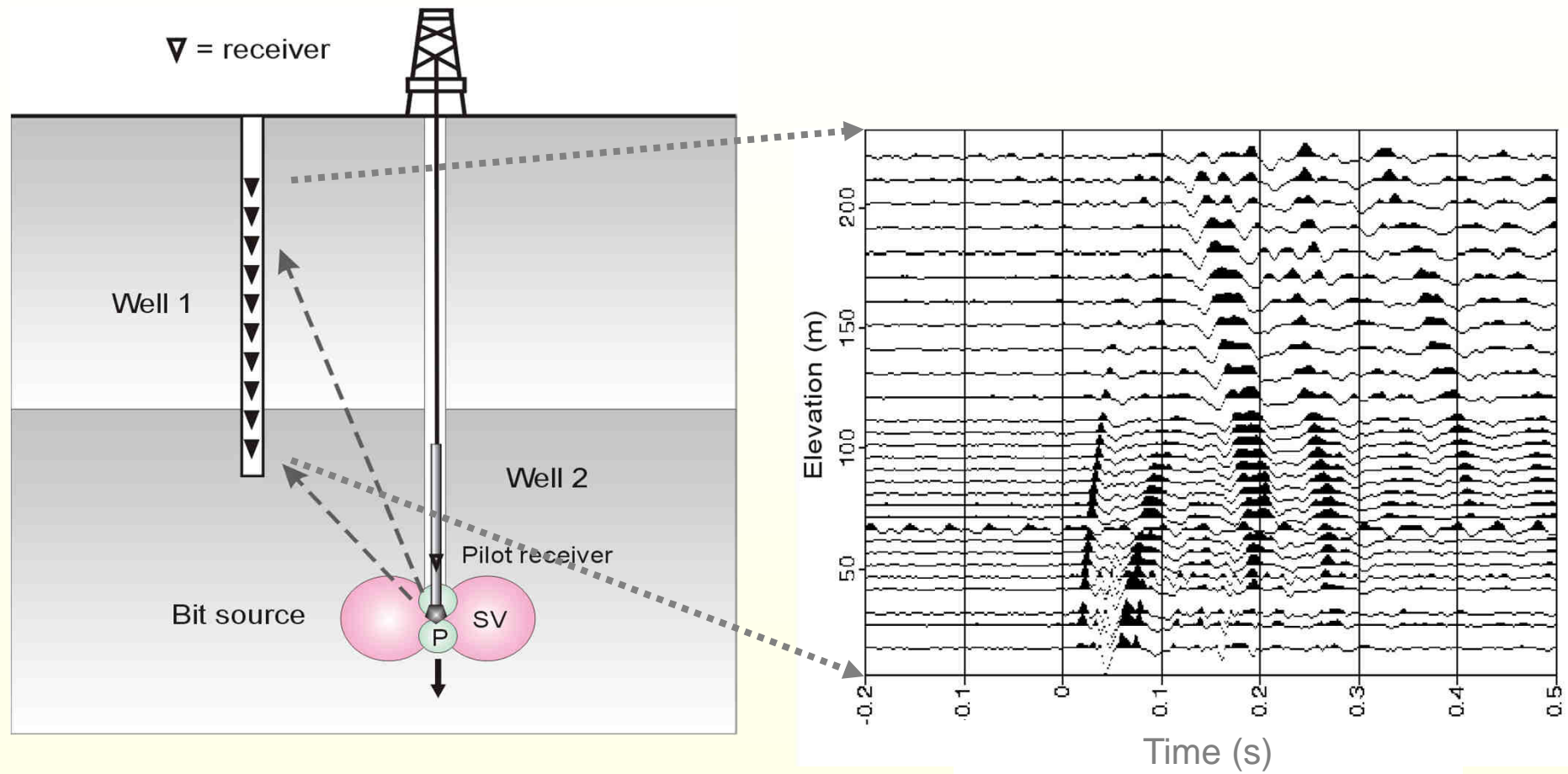


Drill-bit 3D RVSP maps

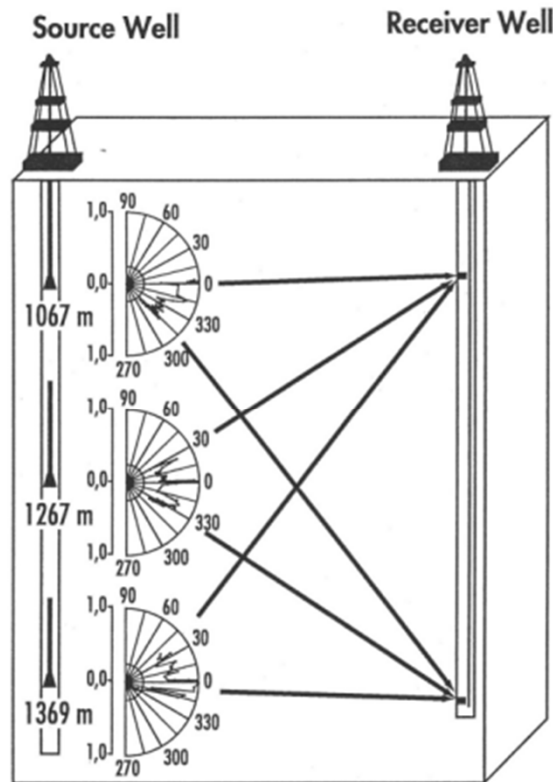
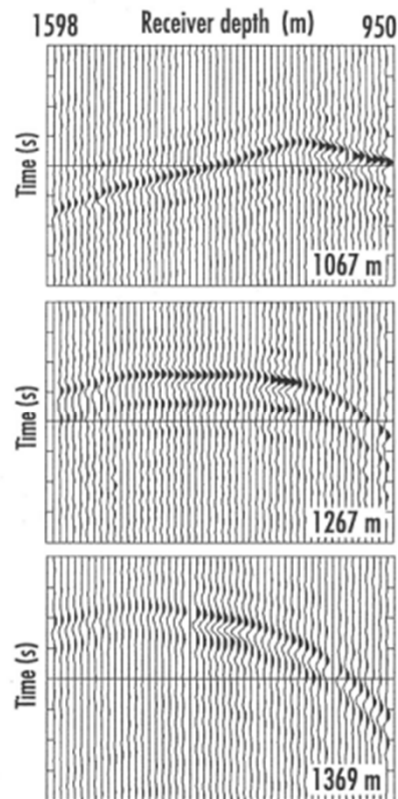


3D imaging by Seismic While Drilling 3D RVSP drill-bit data.
The top of reservoir was identified.

Drill-bit SWD crosshole example

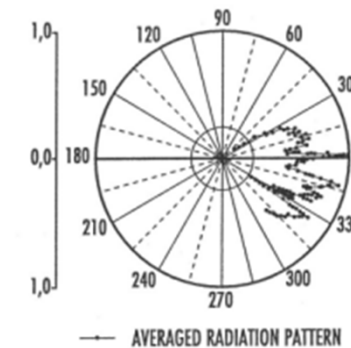


Drill-bit SWD radiation pattern analysis

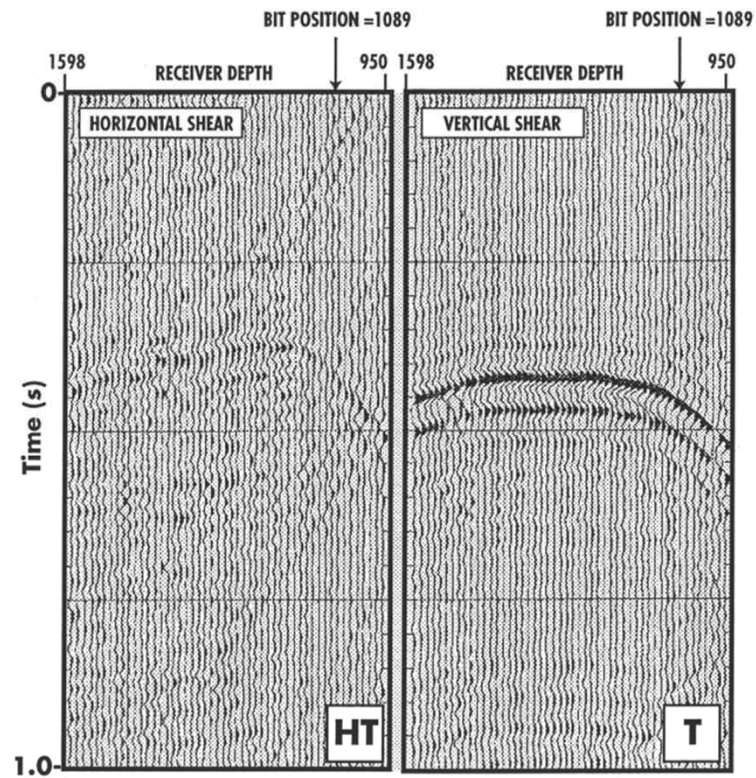


PROCESSING:

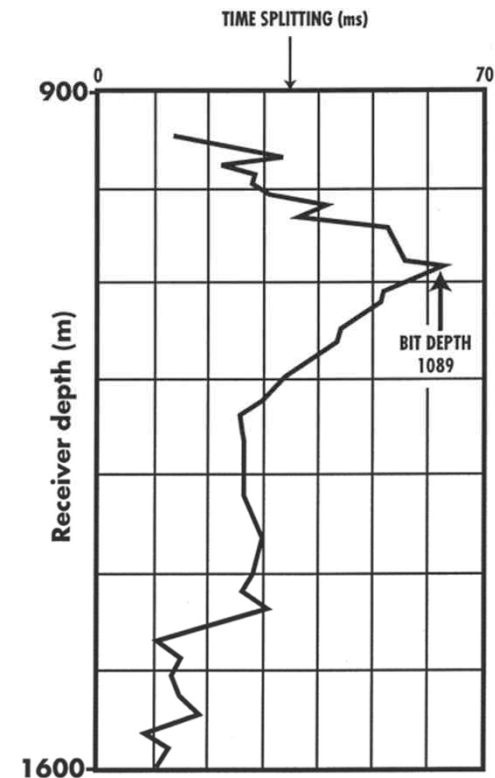
- GEOMETRICAL SPREADING COMPENSATION
- SIMPLIFIED IMPEDANCE RECOVERY
- GEOLOGICAL MODELLING
(no transmission effects, anisotropy assumptions and Q factor compensation)



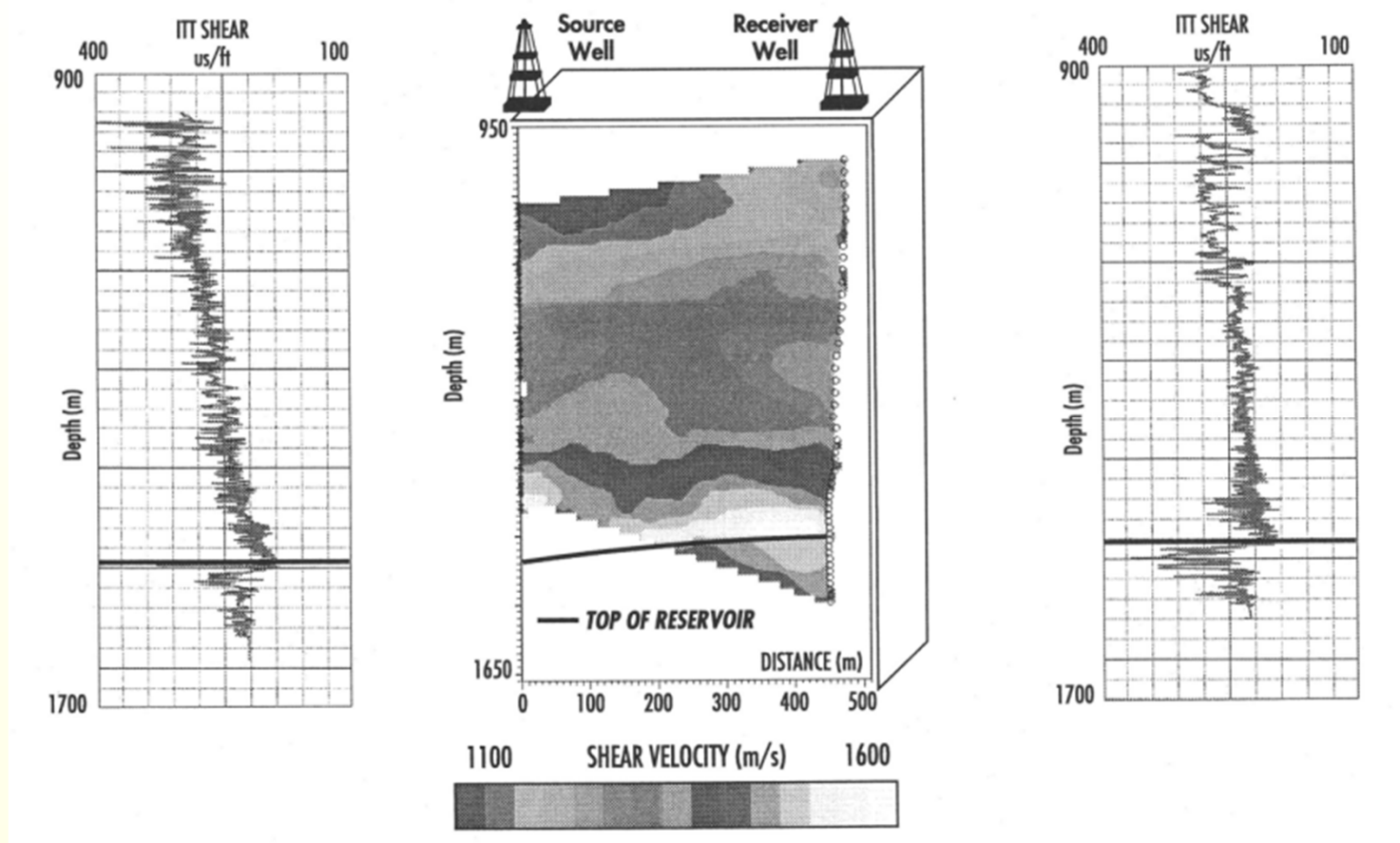
Drill-bit SWD crosswell anisotropy analysis



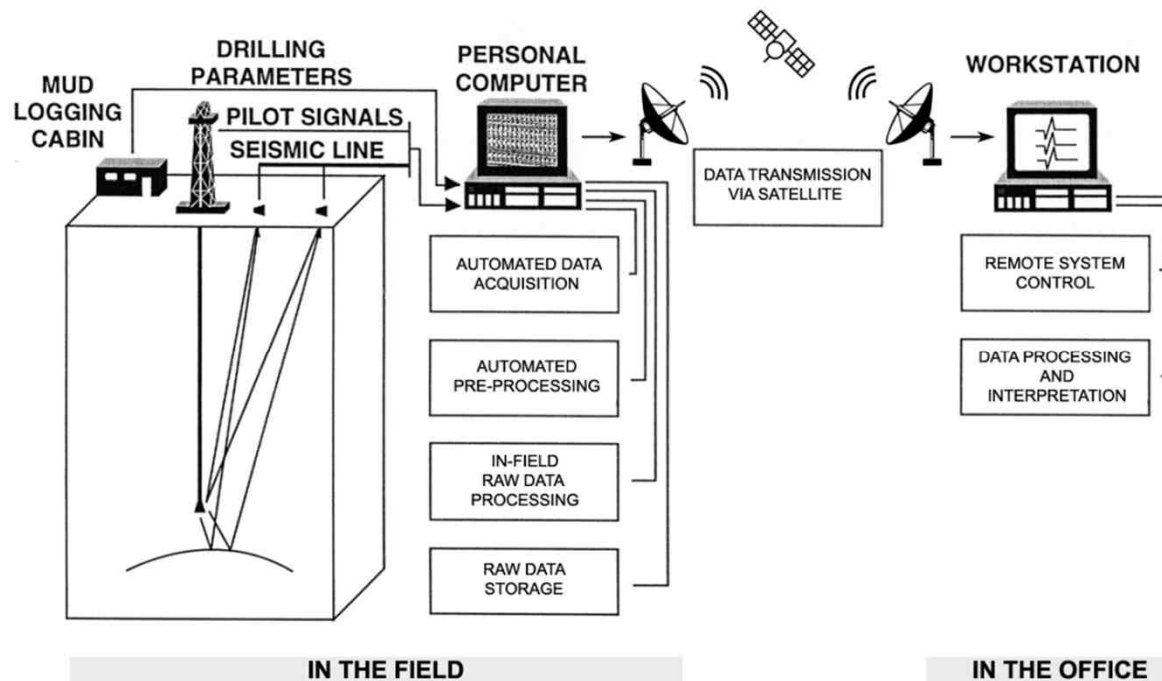
COMMON BIT DEPTH: 1089 m



Drill-bit SWD crosswell tomography



Geothermal SWD application



- Updated SWD technology
- Drilling conditions:
 - Vertical well
 - Medium-hard rock
 - Low ROP
 - Roller cone bit
- Shallow-medium drilling depth (up to 1.0 - 1.5 km)
- SWD by surface sensors only (pilot and seismic signals)

Seismic-while-drilling (SWD) drill-bit method
adapted for geothermal purposes

Geothermal SWD application



- Motivation and target of the SWD survey
- Provide reverse VSP (RVSP) signals using observations from lateral and depth points, approximately 'one way' seismics, useful in complex areas
- Provide while drilling structural information ahead and around the bit (by check shot, velocity maps, SO and MO products typical of SWD)
- Main fault location near and around the drilling path (tune the SWD approach for the characterization of the geothermal zone)
- Extend investigation around the well to obtain areal seismic imaging and improve knowledge of the geothermal-reservoir geological setting

Geothermal SWD scenario

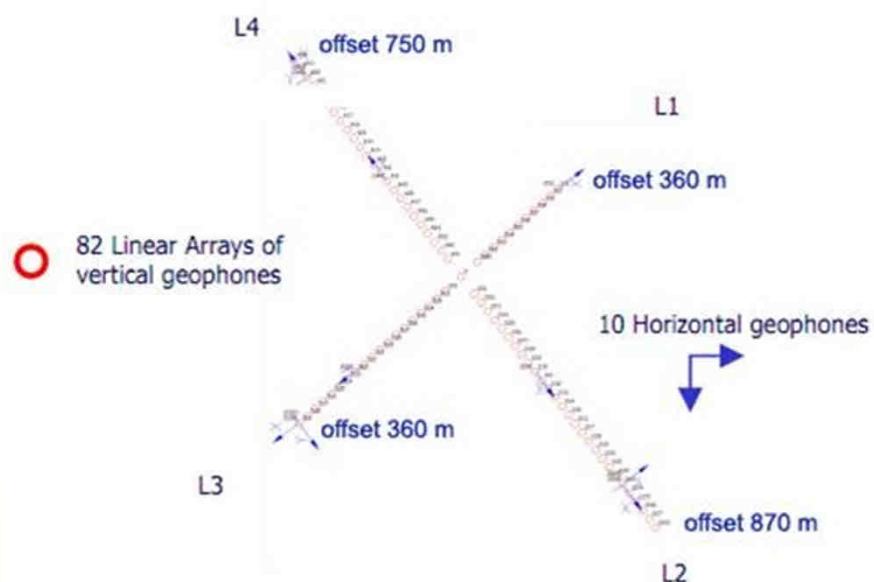


- ❑ Geothermal well location (Nevada, US)
- ❑ Regional trans-tensional system (Walker Lane)
- ❑ Complex fault pattern (main NW-SE strike slip faults + NE-SW normal/synthetic/antithetic/Riedel faults)
- ❑ Well drilled thru gravely-sandy alluvium (siliceous alteration) and rhyolitic ash-flow tuffs

Data used to design the SWD geothermal well survey:

- ❑ Gravity maps
- ❑ CSAMT (Controlled Source Audio frequency Magneto Telluric) data
- ❑ Core holes at nearby locations
- ❑ NO surface seismic data were available

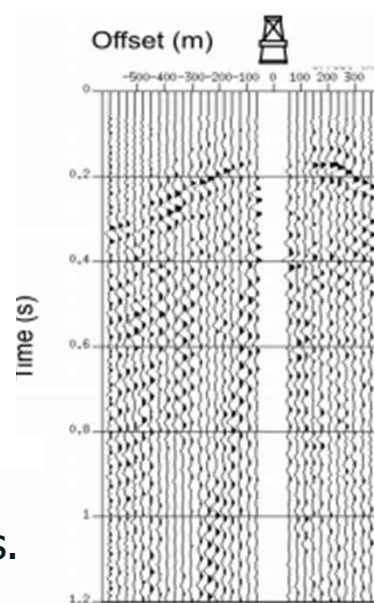
Geothermal SWD acquisition layout



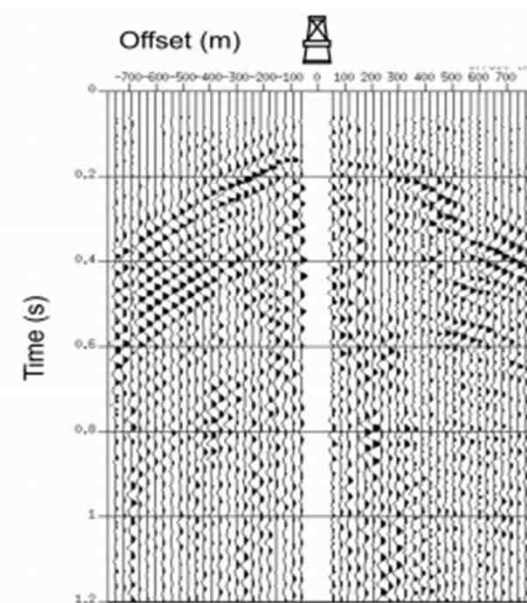
Cross-spread layout of the SWD seismic lines. The inter-trace distance between the vertical-geophone groups is 30 m

- Drilled interval: 180 m to 750 m depth
- Average bit depth interval: 5 m

SWD signals along the seismic lines with the Bit source at depth 290 m

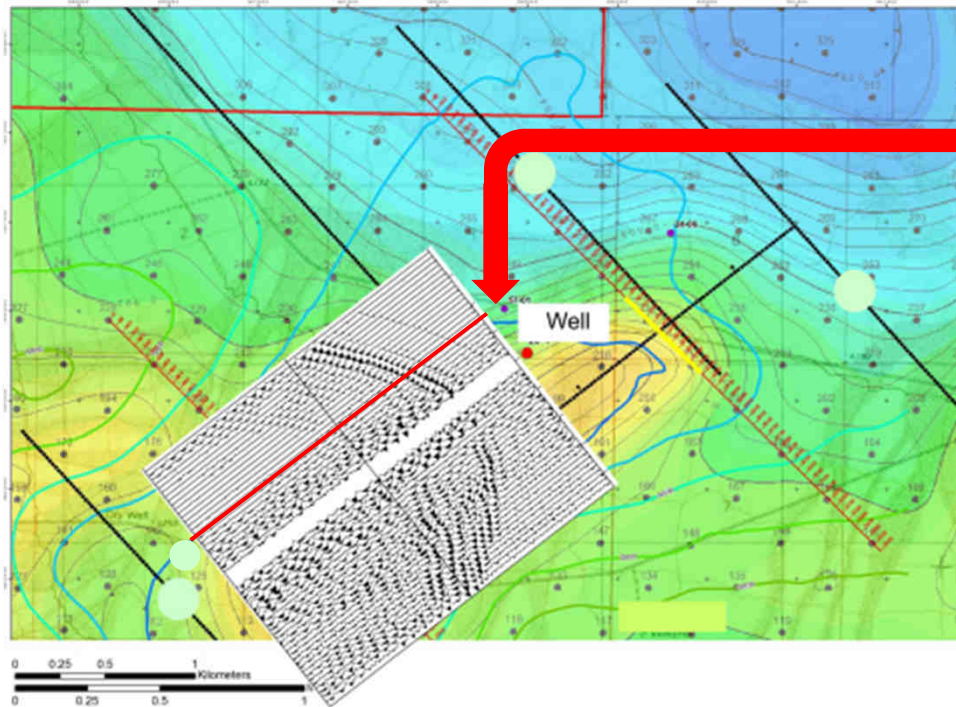


Secondary line (L3-L1) used to control possible lateral effects

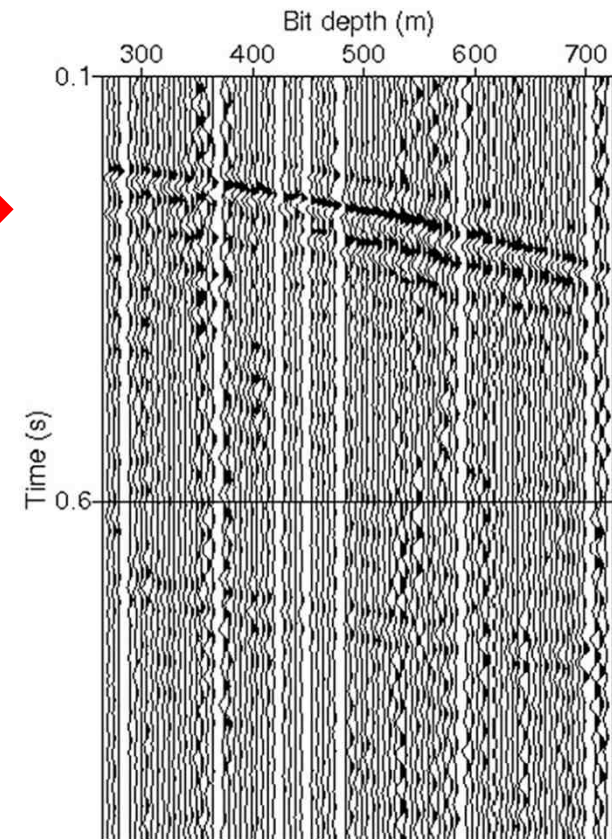


Main line (L4-L2), perpendicular to the principal fault system

Geothermal SWD RVSP gathers

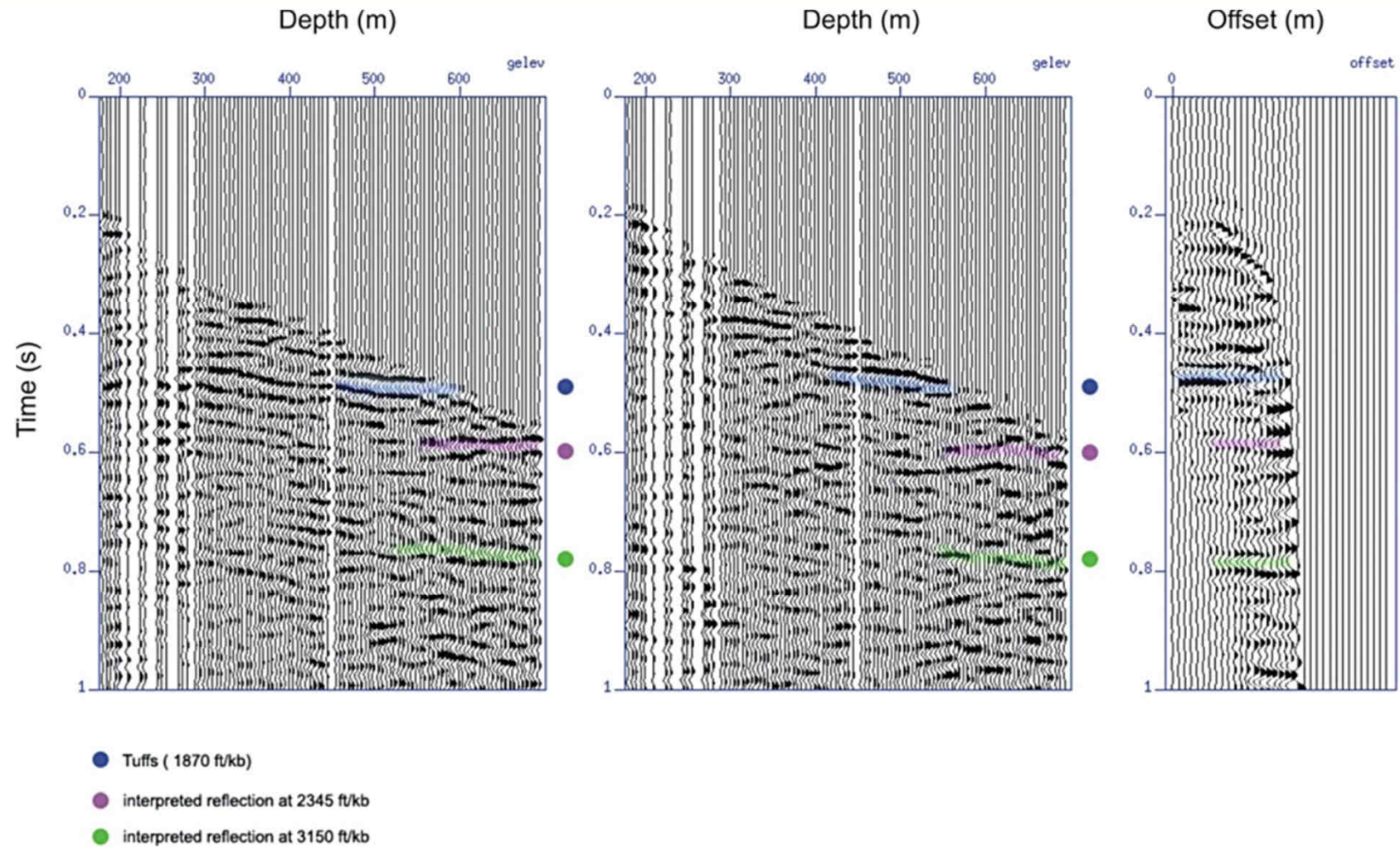


Signal of the main recording line plotted on the gravity map used to plan the survey

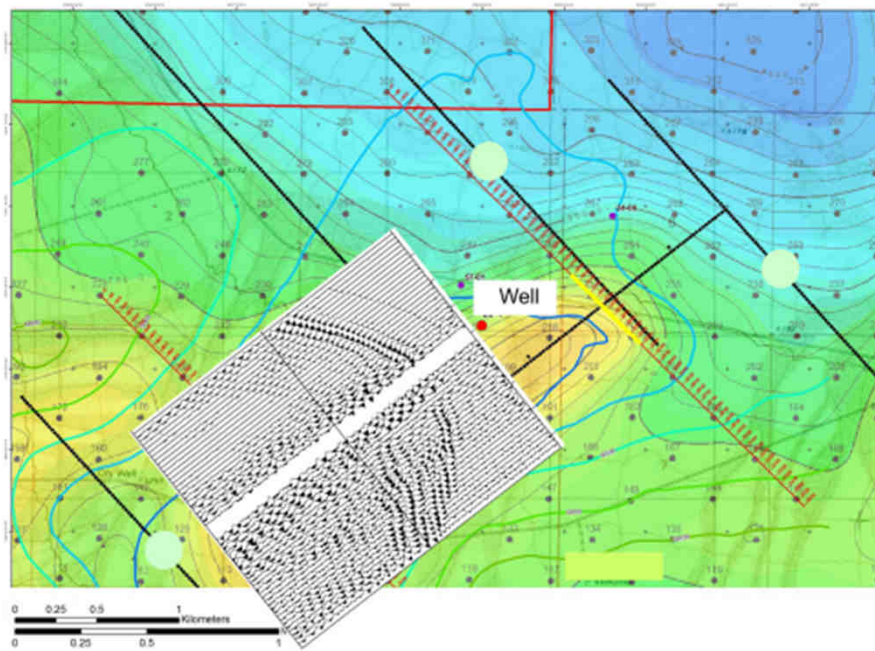


- ❑ Drilled interval: 180 m to 750 m depth
- ❑ Average bit depth interval: 5 m

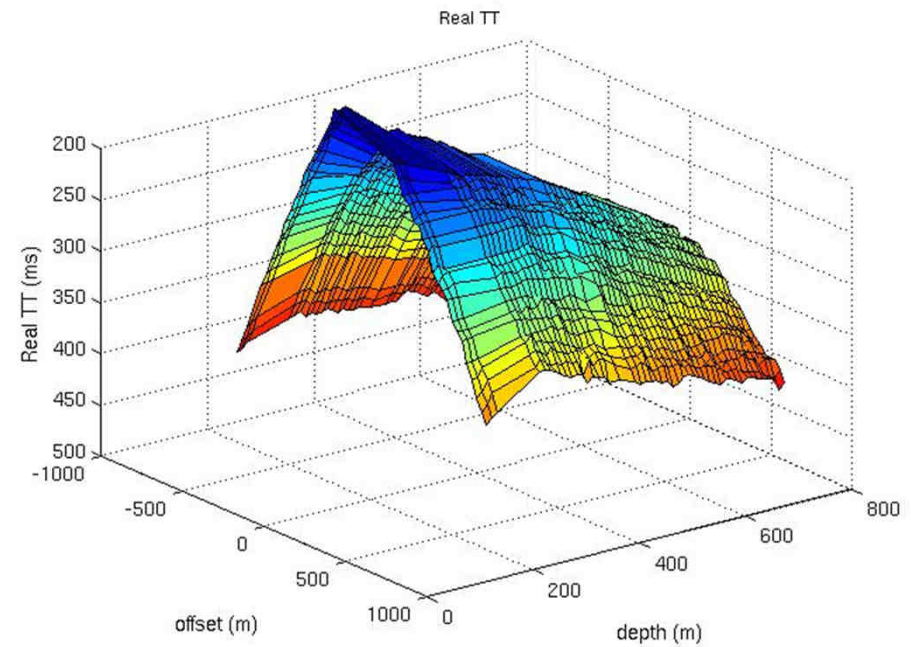
Example of SWD prediction results



Geothermal SWD application



Signal of the main recording line plotted on the gravity map used to plan the survey

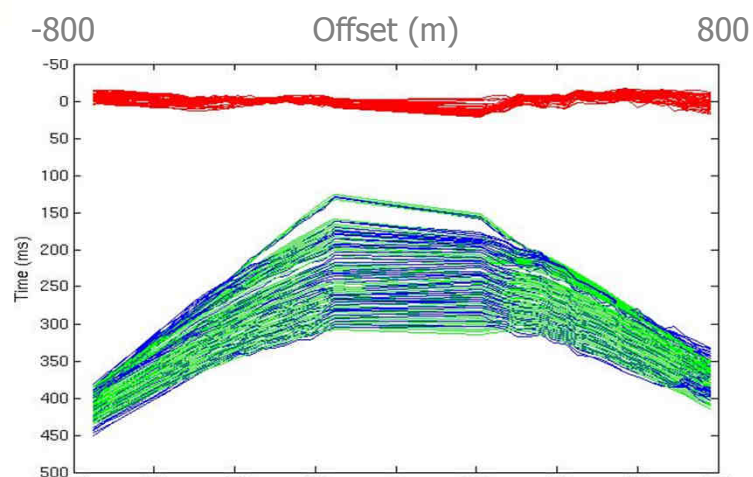


Direct arrivals FB versus offset and depth

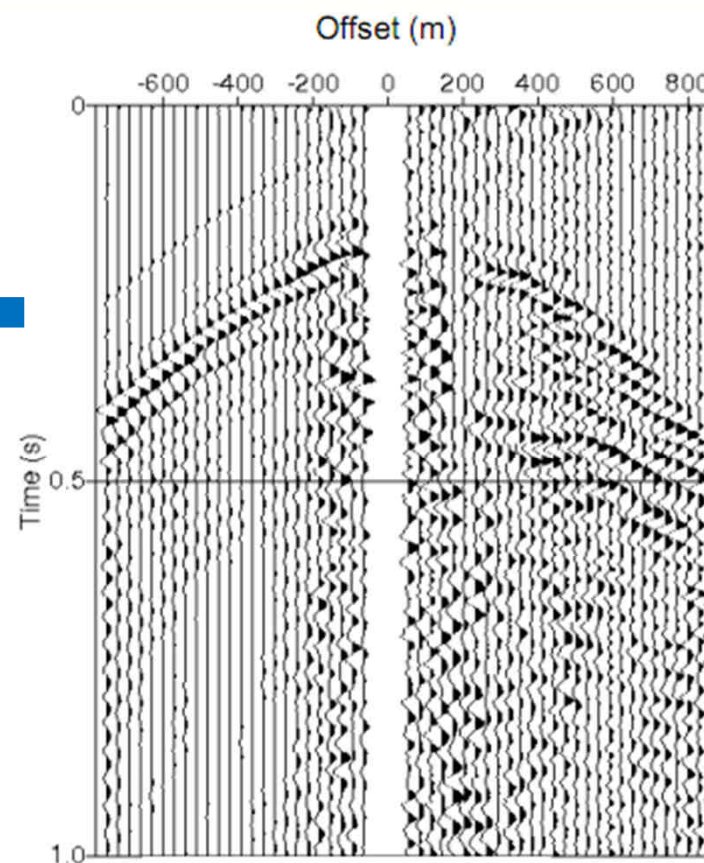
SWD data inversion for migration and imaging



While-drilling (WD) picked and modeled arrival times versus offset (L4-L2)



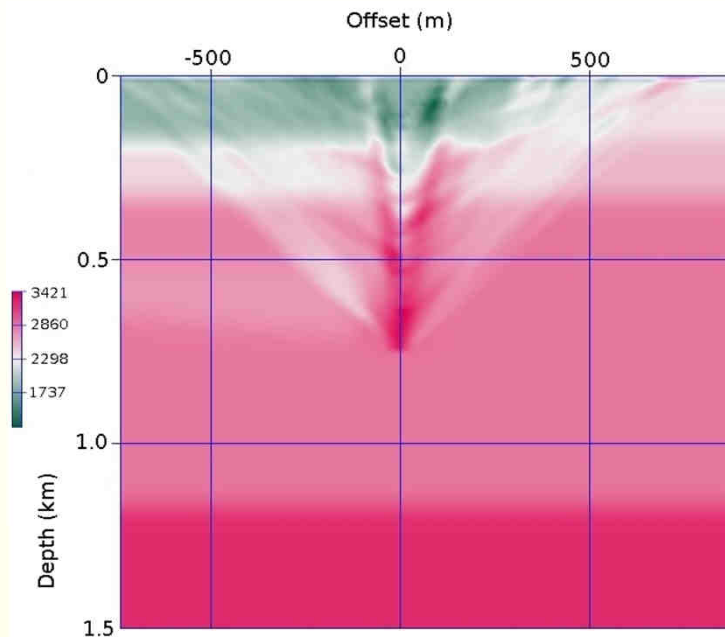
- SWD direct arrivals (blue)
- Model calculated travel times (green)
- Residual time differences (red)



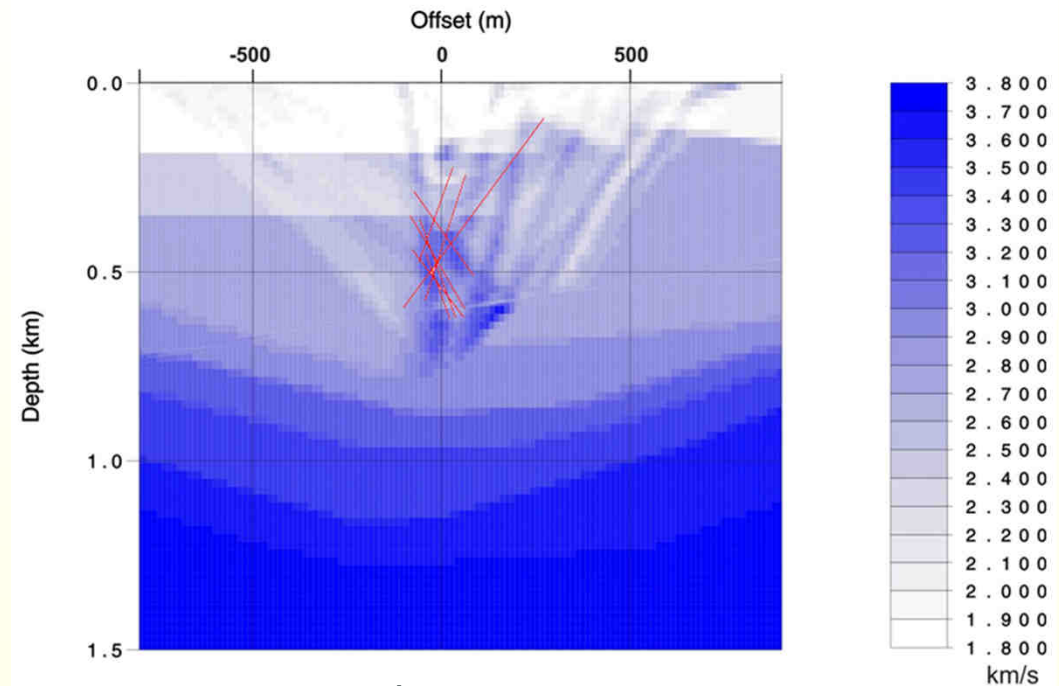
Geothermal SWD application



SWD tomographic inversion for migration and imaging



Tomographic inversion of
SWD direct arrival events

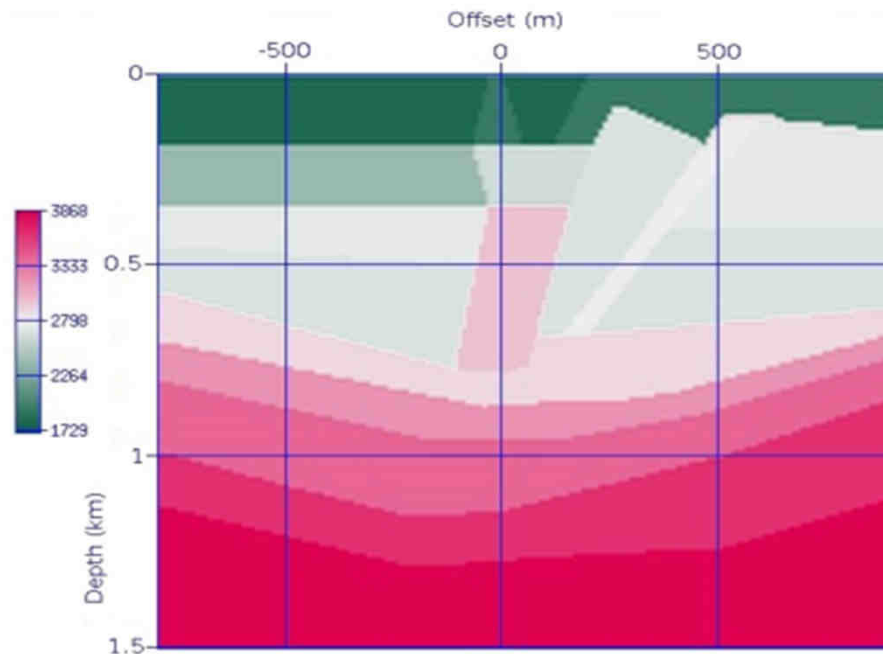


Tomographic joint inversion
of direct and reflected events

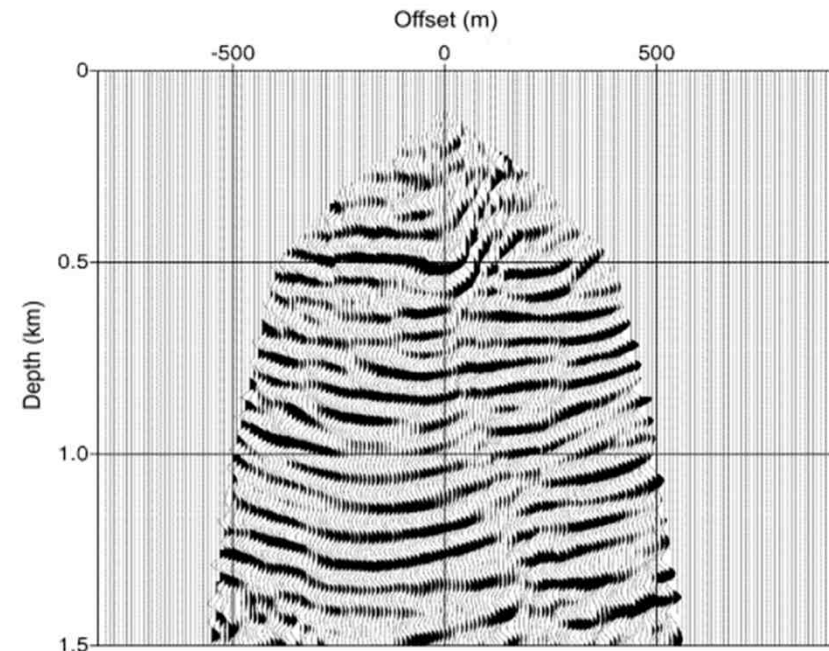
Geothermal SWD application



SWD data migration and imaging



2D velocity model used for migration

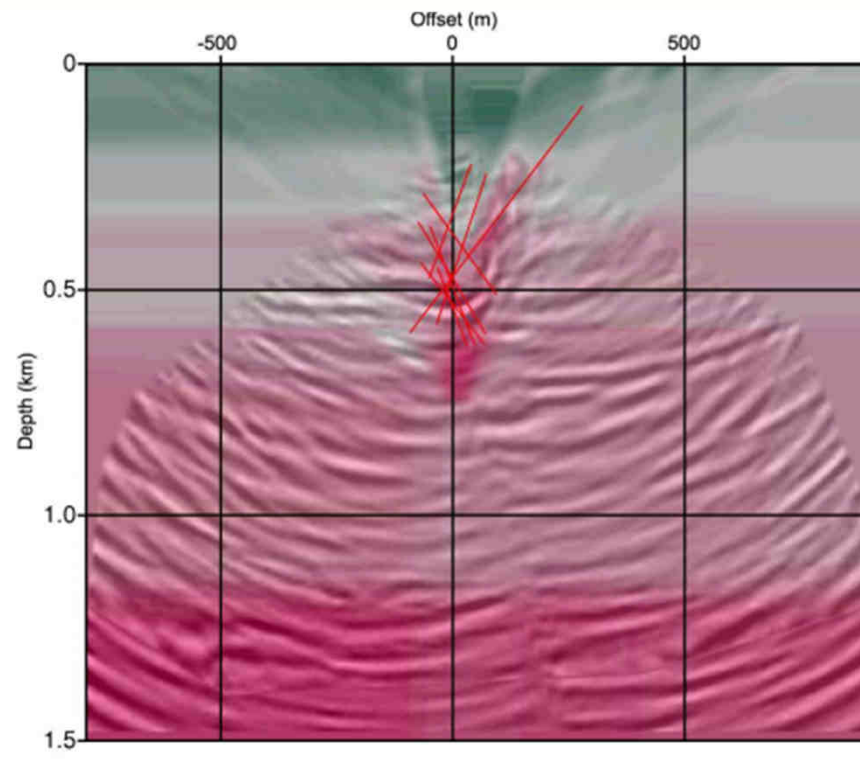


SWD depth migration results

Geothermal SWD application



SWD data migration and imaging: results comparison

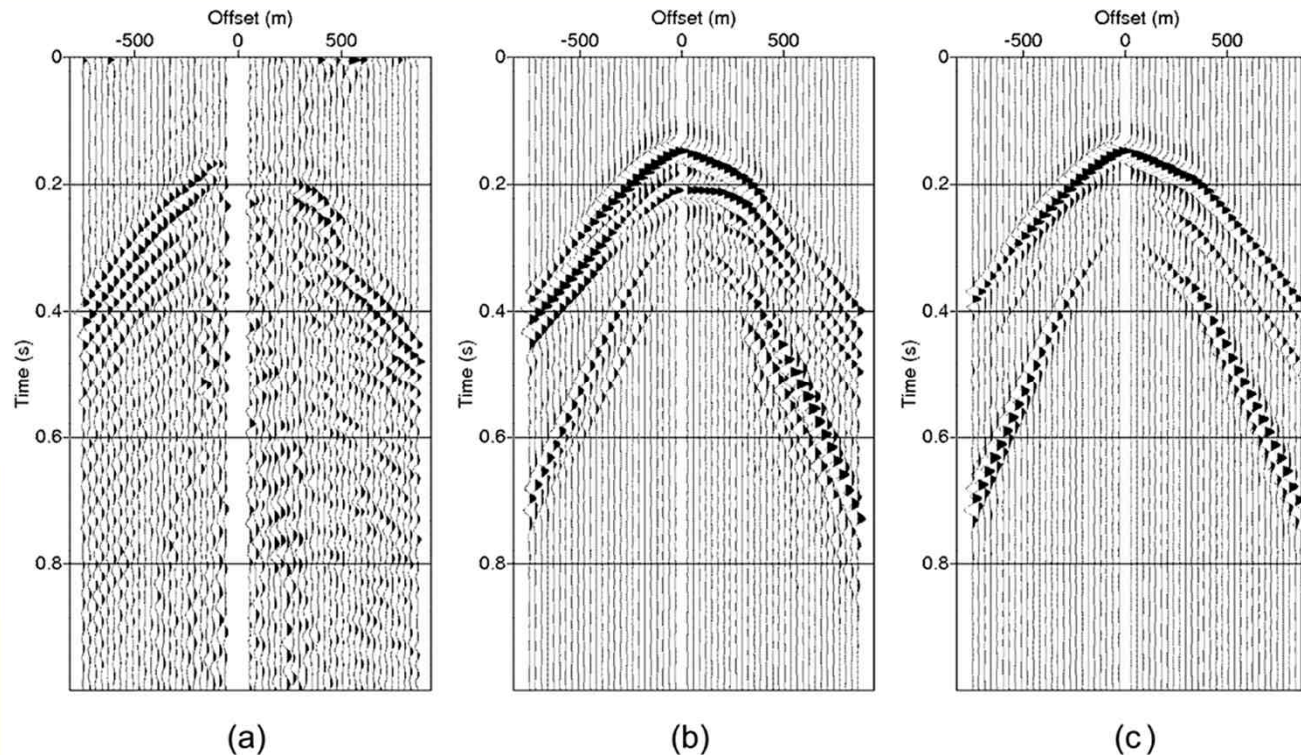


Migration with tomography and
fault system interpretation
(using drilling results)

Geothermal SWD application



SWD FW data analysis of fault's response

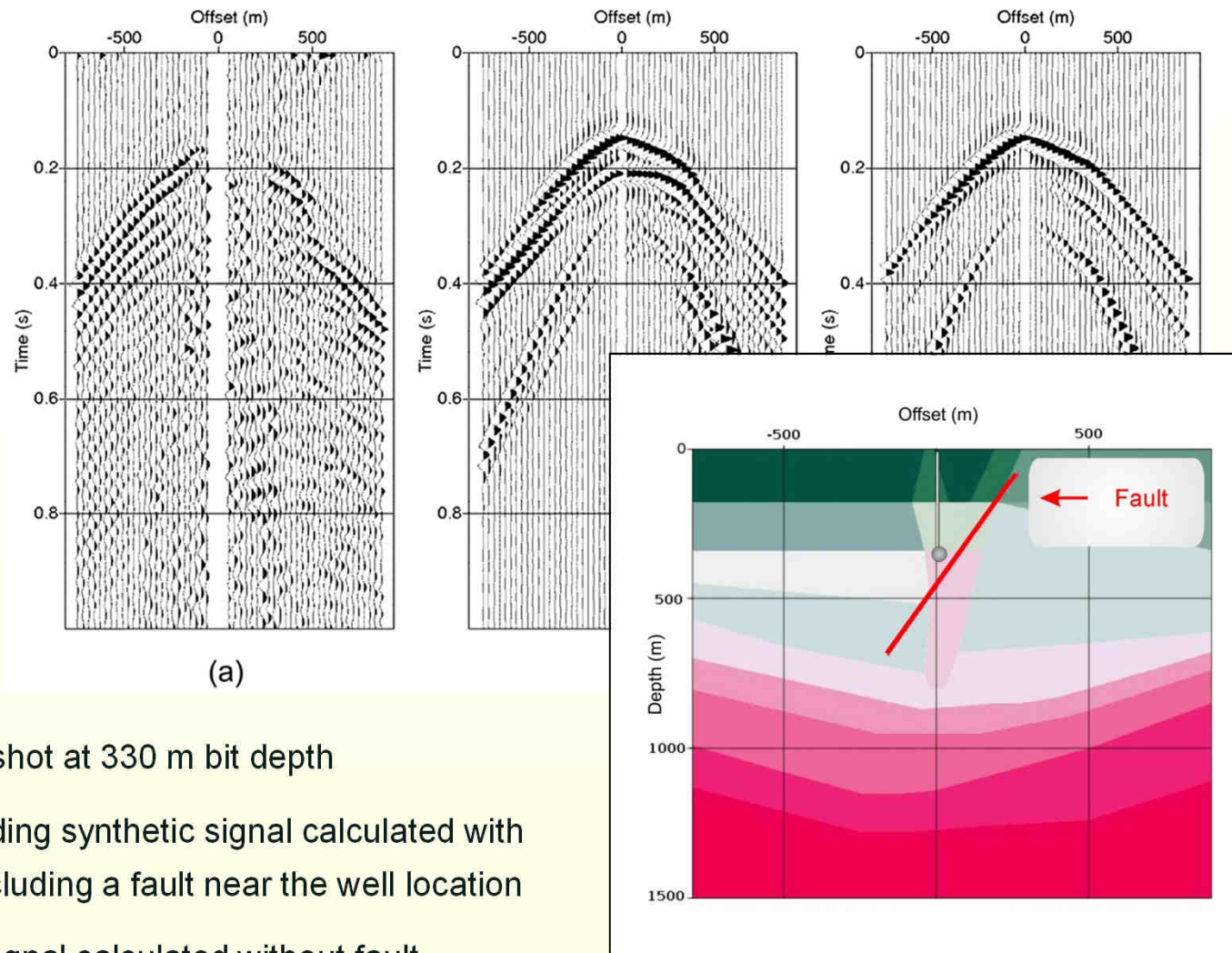


- a) SWD field shot at 330 m bit depth
- b) Corresponding synthetic signal calculated with a model including a fault near the well location
- c) Synthetic signal calculated without fault

Geothermal SWD application



SWD FW data analysis of fault's response

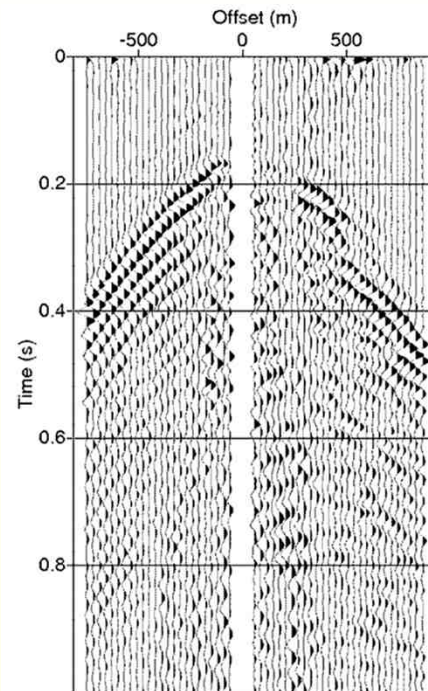


- a) SWD field shot at 330 m bit depth
- b) Corresponding synthetic signal calculated with a model including a fault near the well location
- c) Synthetic signal calculated without fault

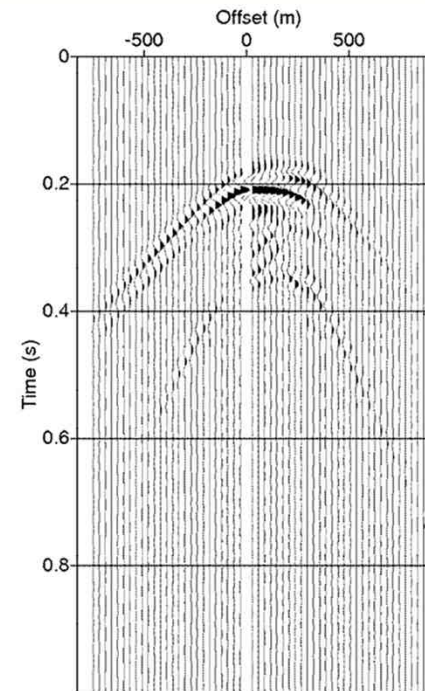
Geothermal SWD application



SWD FW data analysis of fault's response



SWD field shot



Synthetic fault response

Geothermal SWD application



Advantages of Drill-bit SWD for geothermal purposes

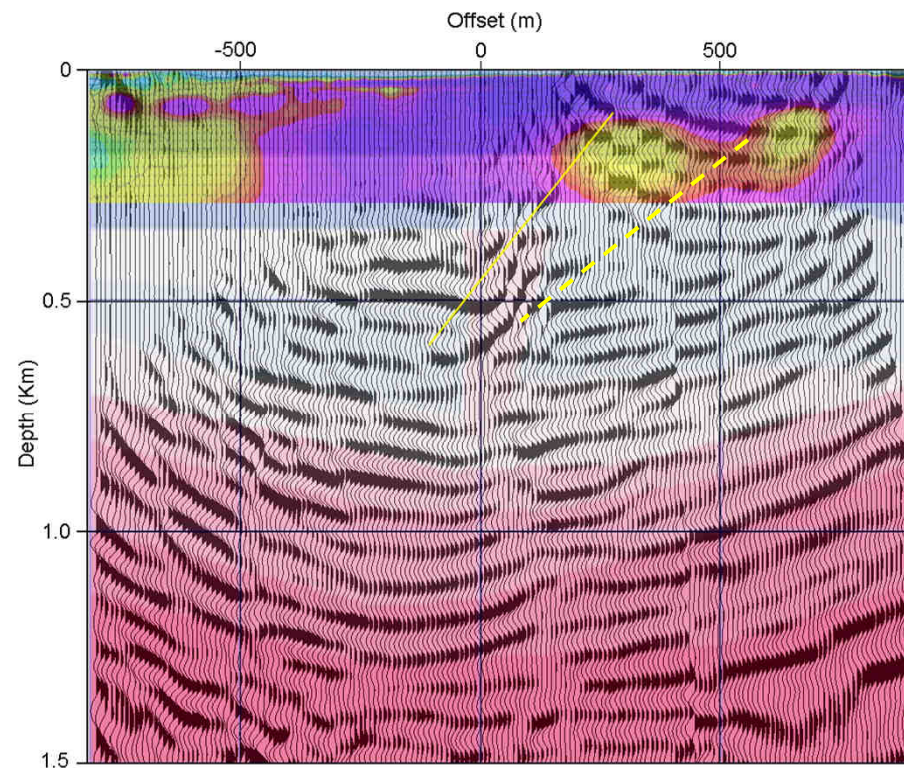
Drill bit as a WD seismic source, summary of advantages:

- ❑ Passive method, while-drilling geophysical survey without interference with drilling activity
- ❑ No need of recording tools in the HT well
- ❑ Allows to extend lateral information using surface seismic lines around the well
- ❑ Important WD information about subsoil settings and structural variations contained in raw drill-bit data
- ❑ Potential WD products: joint inversion of seismic travel times and gravity data
- ❑ Integration with prediction and imaging to support geothermal exploration from seismic point of view

Geothermal SWD application



Drill-bit seismic data integrated interpretation



Combination of tomography, RVSP SWD migration, SWD interferometry (see Poletto et al., SEG 2011), with fault interpretation and with TEM results on the top

Conclusions

- ❑ Drill-bit SWD method was applied without support of surface seismic information
- ❑ Main results consist in WD geophysical products, interpretation of faults and discontinuities, imaging
- ❑ Raw field data (shots) contain significant information for WD fault interpretation
- ❑ Integration with surface refraction and shallow seismic reflection survey recommended for future applications
- ❑ Future work: method tuning to further optimize SWD products and costs for geothermal purposes

Part 2 - Seismic interferometry



- ☐ SWD concept
- ☐ SWD using the drill-bit source
- ☐ Examples

- ☐ Introduction to seismic interferometry (SI)
- ☐ Concepts and applications
- ☐ Multidimensional wavefield representation

Seismic interferometry



Synthesis of Virtual seismic signals

Virtual seismic signals are synthesized by processing (cross-composing and stacking) seismic traces recorded by a plurality of real sources and receivers

- ❑ **Seismic Interferometry (SI)** method uses crosscorrelation to compose the recorded traces (e.g., Wapenaar, 2004; Schuster, 2009), and to get virtual sources at the position of receivers (Calvert, 2004; Bakulin et al., 2007)

- ❑ **Virtual Reflector (VR)** method uses crossconvolution to simulate virtual reflectors (Poletto and Farina, 2008; Poletto and Wapenaar, 2009) at the position of the recording line

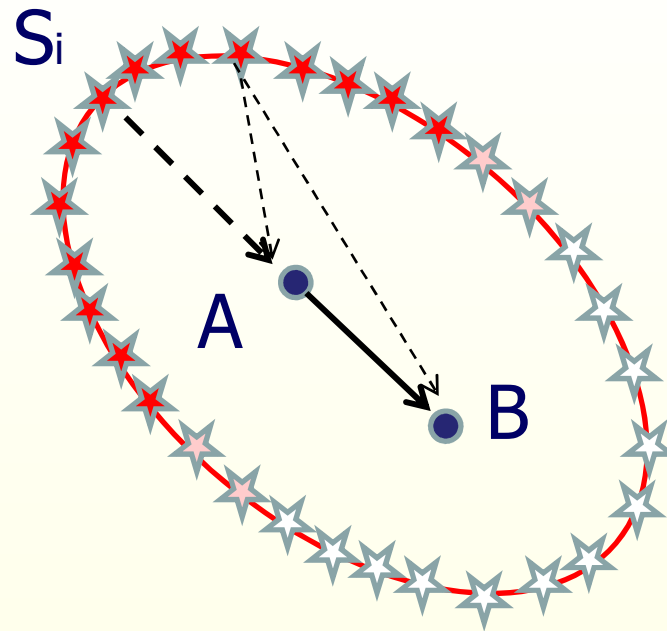
These methods do not need knowing the subsurface velocity model.

Seismic interferometry



Synthesis of Virtual sources

- Receiver
- ★ Real source



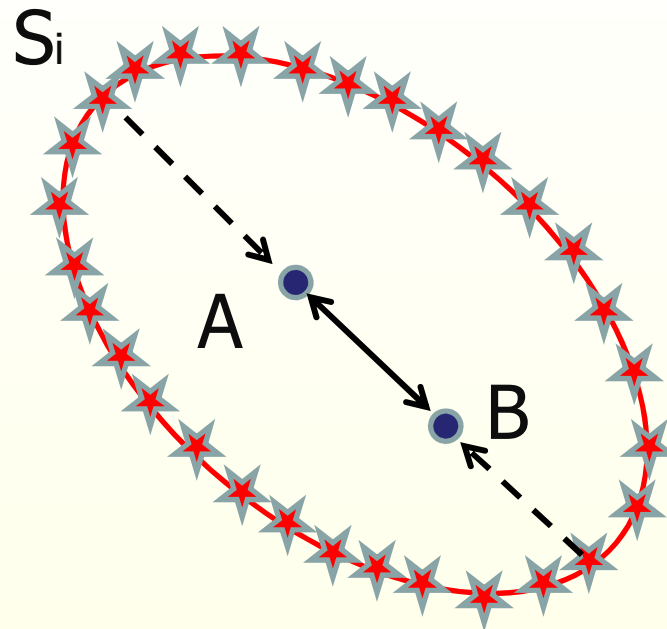
In the frequency domain $x_{BA} \cong \sum_i x_{B,i} x_{A,i}^*$

Seismic interferometry



Synthesis of Virtual sources

- Receiver
- ★ Real source



In the frequency domain

$$x_{BA} + x_{AB}^* \cong \sum_i x_{B,i} x_{A,i}^*$$

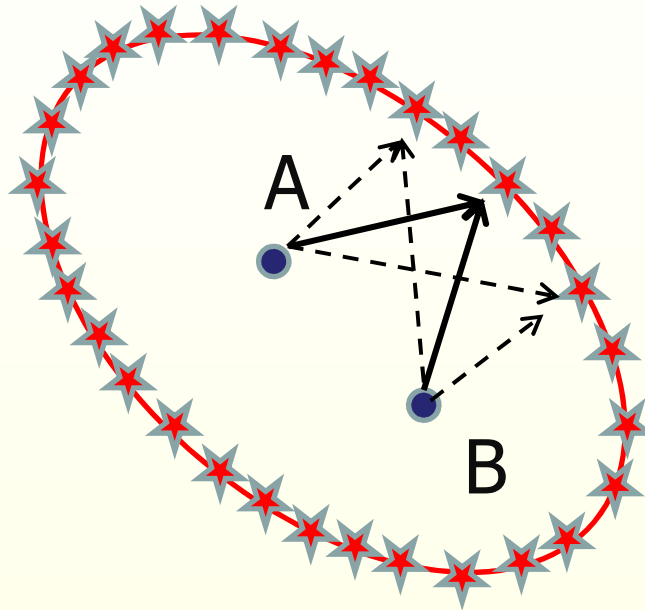
Seismic interferometry



Synthesis of Virtual Reflector (by convolution)

● Source (receiver)

★ Receiver (source)



In the frequency domain $x_{AB} = x_{BA} \cong \sum_i x_{B,i} x_{A,i}$

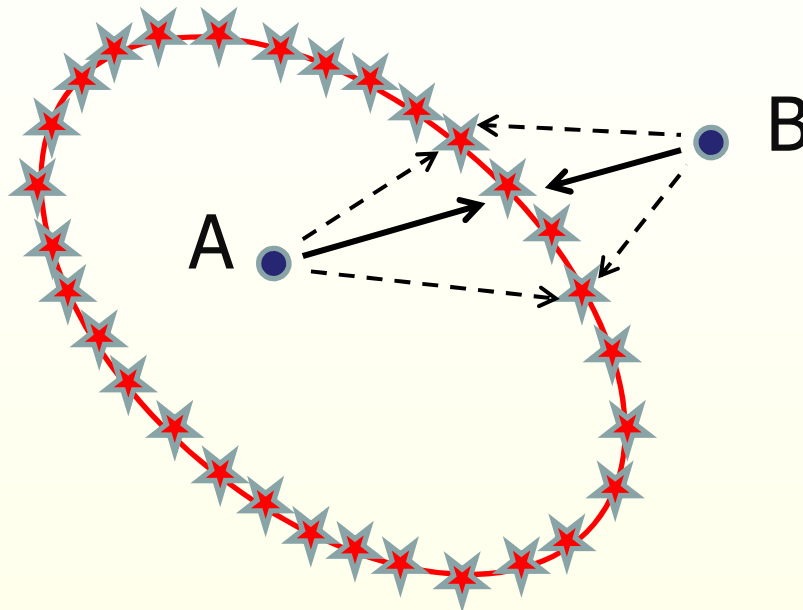
Seismic interferometry



Extrapolation outside the domain (by convolution)

● Source (receiver)

★ Receiver (source)

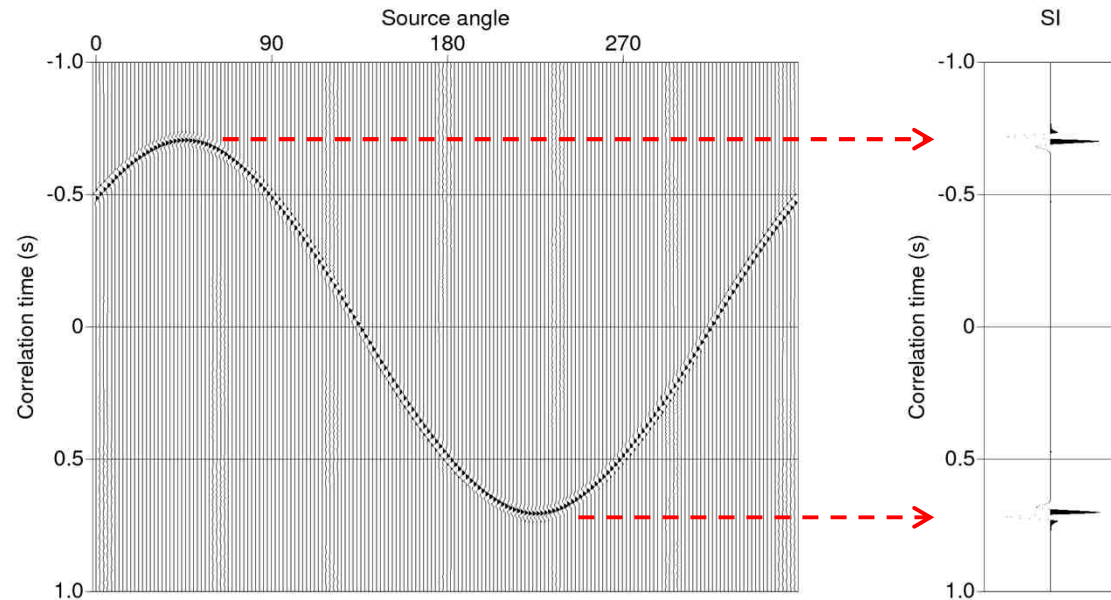
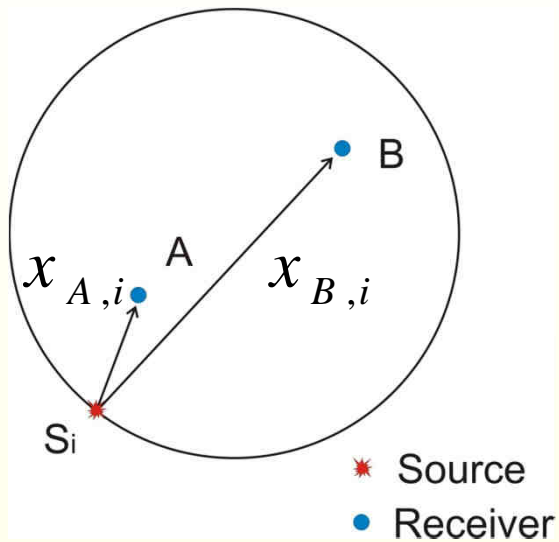


In the frequency domain $x_{AB} = x_{BA} \cong \sum_i x_{B,i} x_{A,i}$

Seismic interferometry



Illumination and stationary phase for virtual sources



$$x_{B,i} x_{A,i}^*$$

$$\sum_i x_{B,i} x_{A,i}^*$$

Acoustic Green's function representation



Acoustic model used for interferometry representation

x_A =receiver position

x_B =receiver position

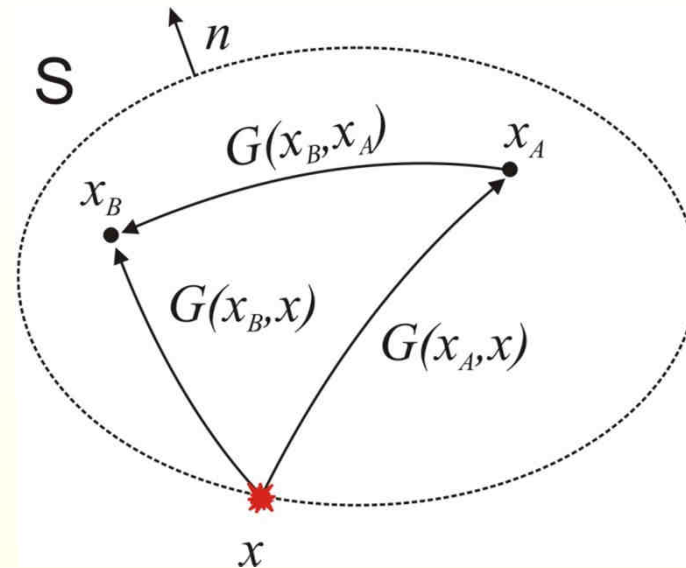
x =source position

S =bounding surface

n =outward normal to S

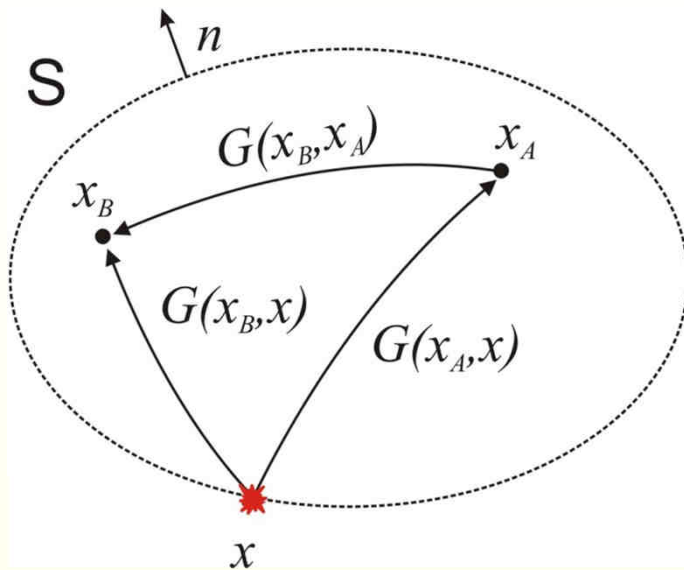
$G(x_B, x_A)$ =Green's function from x_A to x_B

$G(x_A, x)$ =Green's function from x to x_A



Assume a homogeneous
medium outside S

Seismic interferometry acoustic representation (by reciprocity theorem of correlation type)



Integration is performed on the source space \mathbf{S} to synthesize a virtual seismic source at a receiver position

$$G(x_A, x_B, \omega) + G^*(x_B, x_A, \omega) = \frac{-1}{4\pi i \omega} \int_S dS \left[G^*(x_A, x, \omega) \frac{\partial G(x_B, x, \omega)}{\partial n} - G(x_B, x, \omega) \frac{\partial G^*(x_A, x, \omega)}{\partial n} \right]$$

(modified after Wapenaar and Fokkema (2006))

where $*$ denotes complex conjugate and we assume unit mass density

SI acoustic representation



Taking into account the contributions at the stationary points, using the approximation $\frac{\partial}{\partial n} \cong -i\omega \cos \gamma / c$ for the normal derivative, and using reciprocity, we can express the SI representation as

$$G(x_A, x_B, \omega) + G^*(x_A, x_B, \omega) = \frac{1}{2\pi c} \int_S G(x_B, x, \omega) G^*(x_A, x, \omega) \cos \gamma dS$$

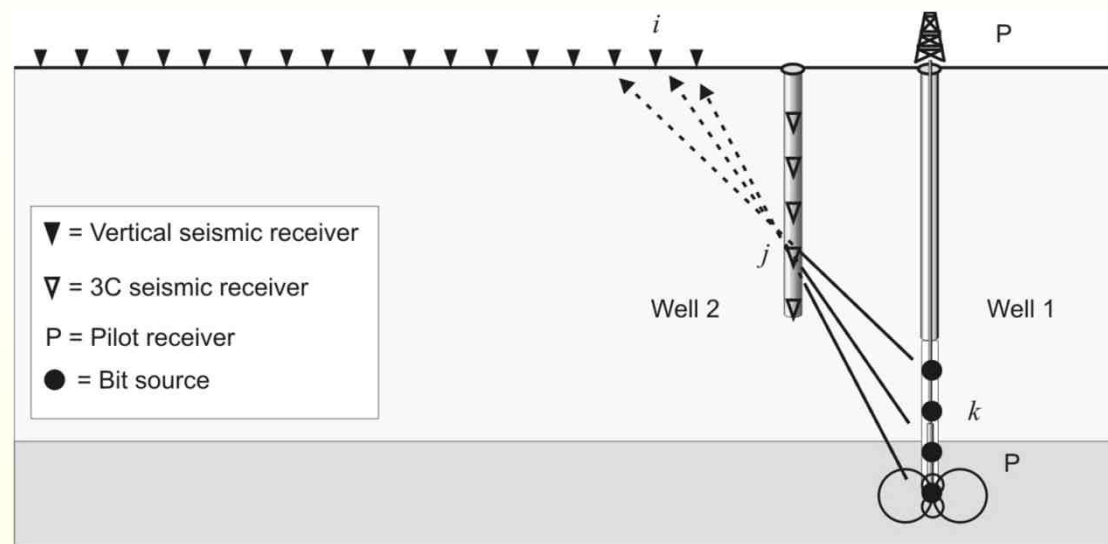
and, if we assuming normal-ray incidence ($\gamma = 0$), we obtain the crosscorrelation representation by

$$G(x_A, x_B, \omega) + G^*(x_A, x_B, \omega) = \frac{1}{2\pi c} \int_S G(x_B, x, \omega) G^*(x_A, x, \omega) dS$$

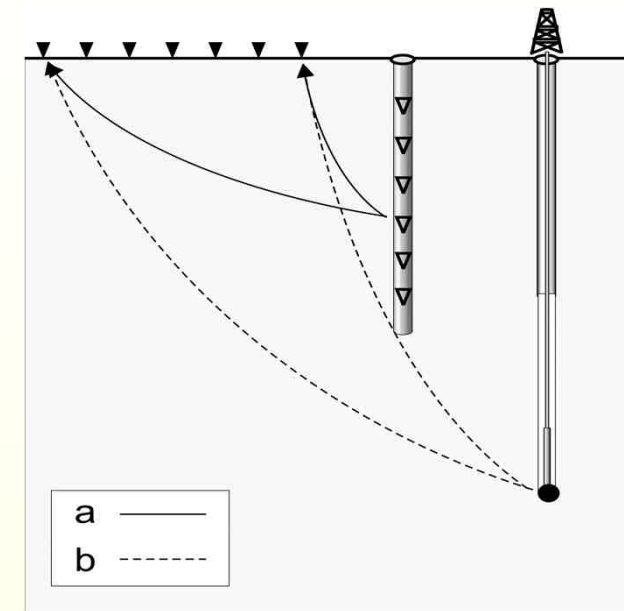
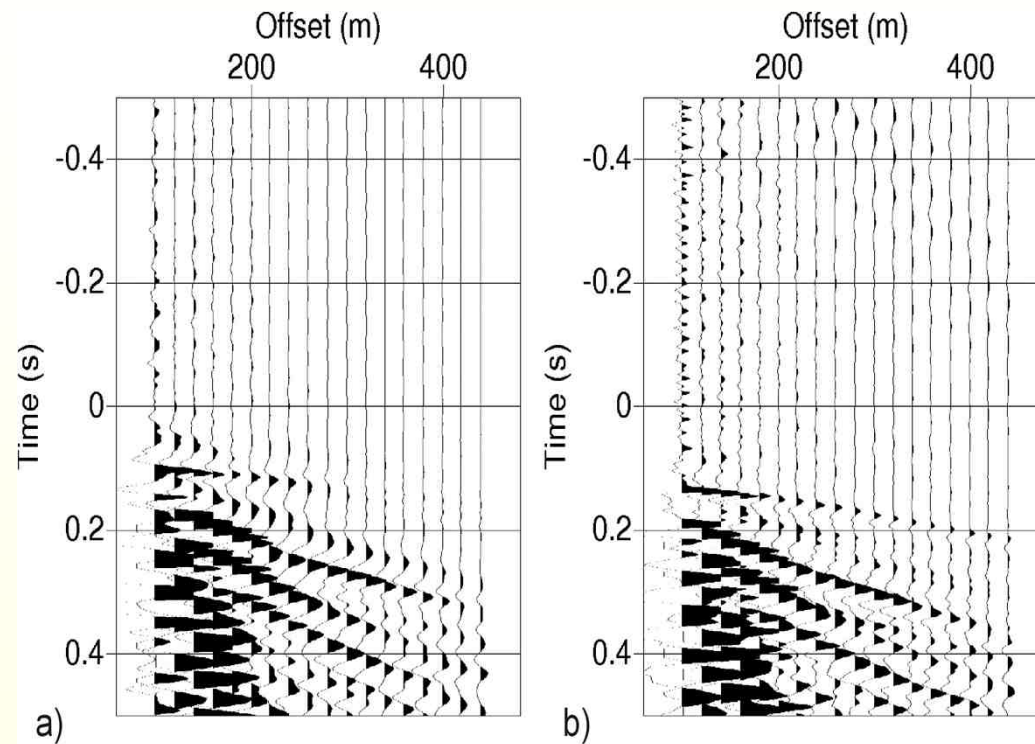
SWD SI application: example 1



□ SWD interferometry using pilot-correlated signals



Drill-bit SWD interferometry



Interferometry vs conventional SWD

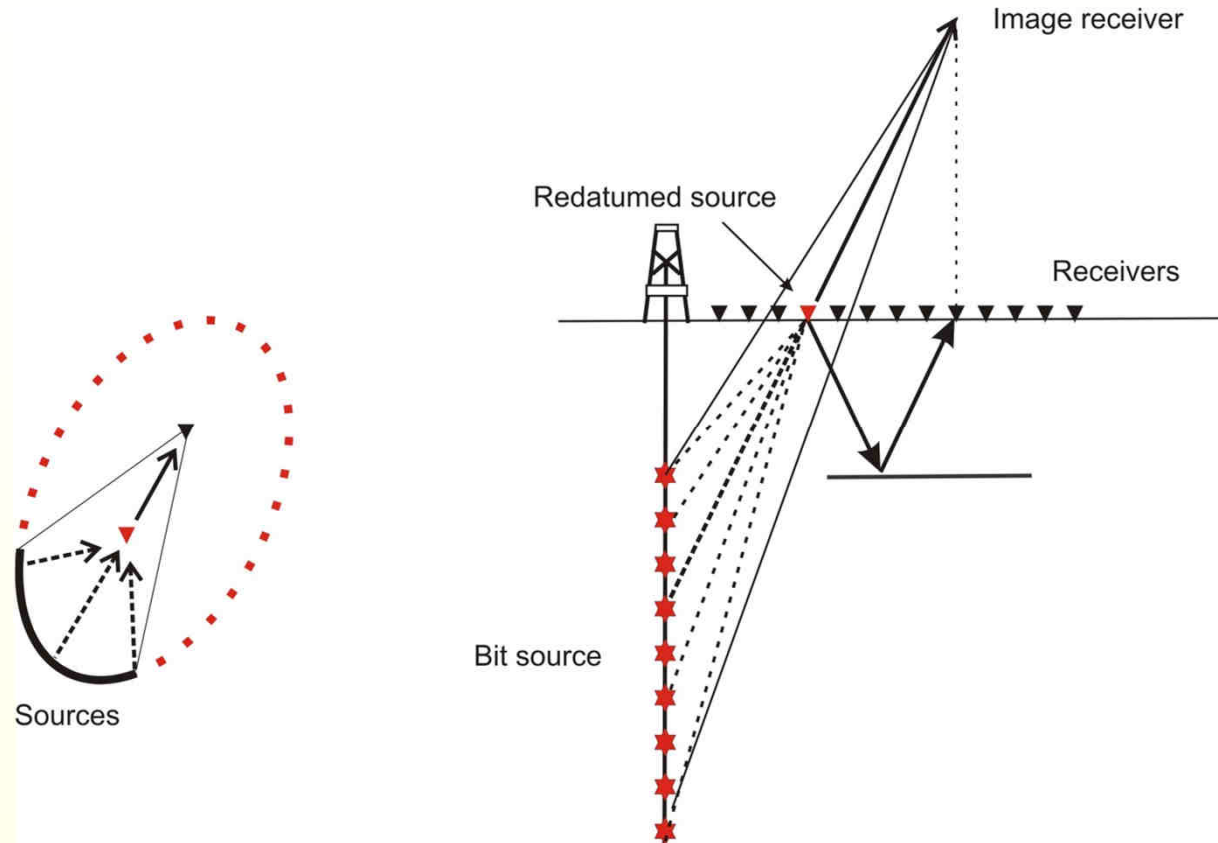
Poletto et al. (2011) Geophysical Prospecting

Applications: example 2



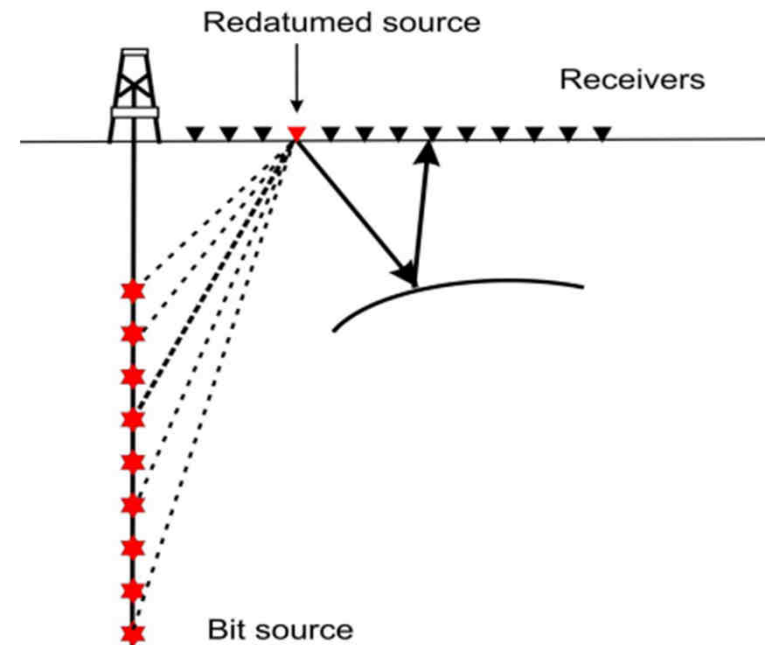
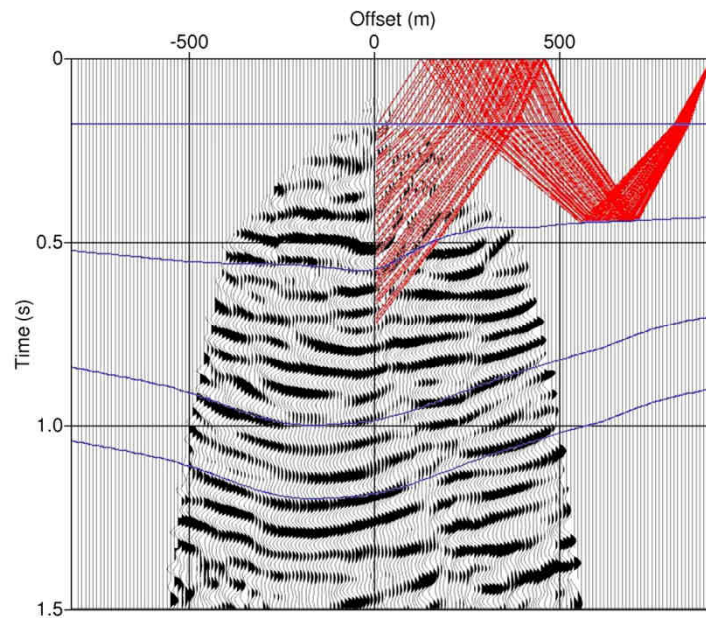
- ☐ SWD geothermal application
- ☐ Use SWD interferometry to extend lateral coverage
- ☐ Use SWD interferometry to extend shallow coverage

Applications: example 2



Concept of seismic interferometry application for drill-bit SWD purposes: to crosscorrelate signals at different receivers and stack over the source domain to obtain an estimate of the Green's function between receivers

Applications: example 2



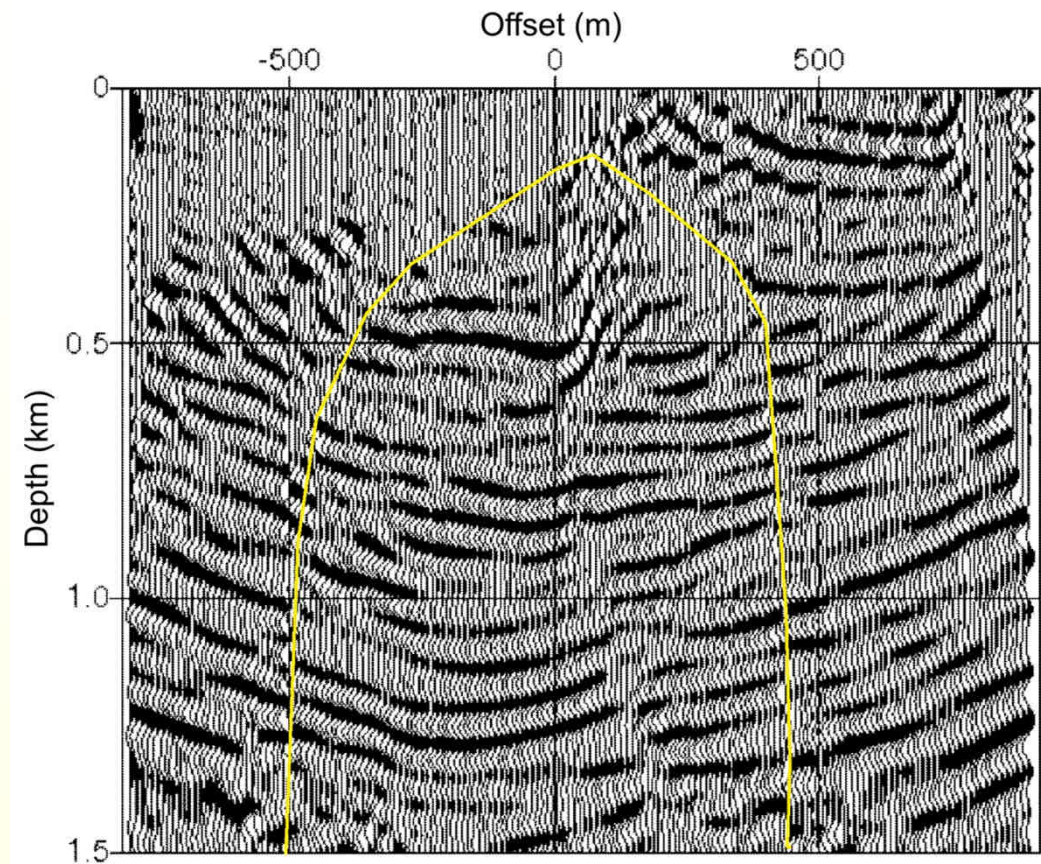
Concept of seismic interferometry application for drill-bit SWD purposes

Drill-bit RVSP and seismic interferometry migration



SWD seismic interferometry migration:

- Calculation of seismic interferometry using drill-bit SWD RVSP signals (no need of seismic model)
- Migration of the interferometry results using the same model of the SWD RVSP migration

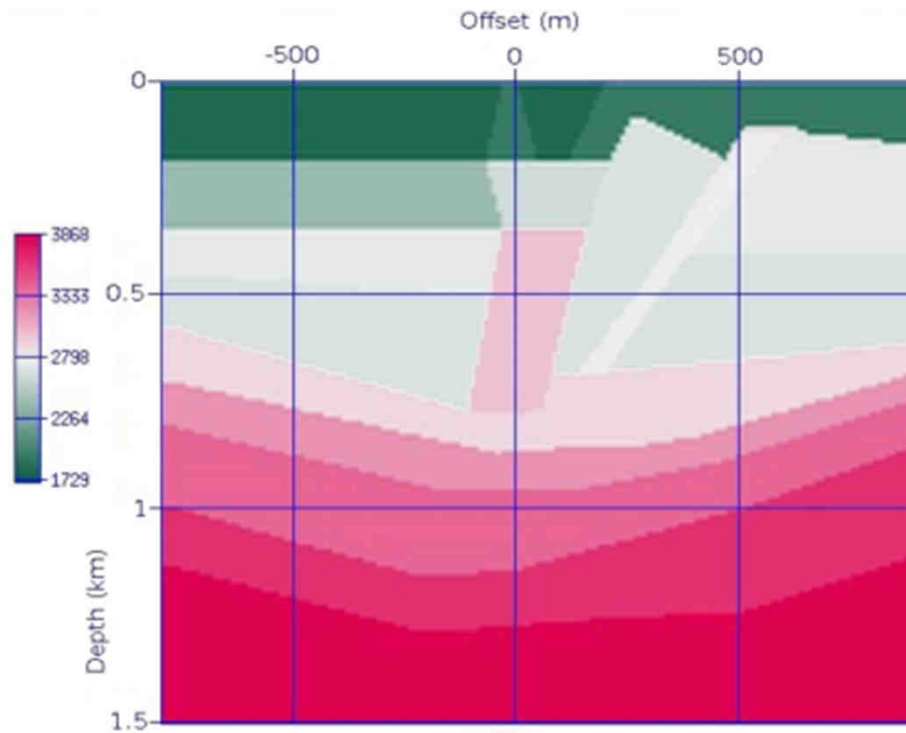


Interferometry
migration

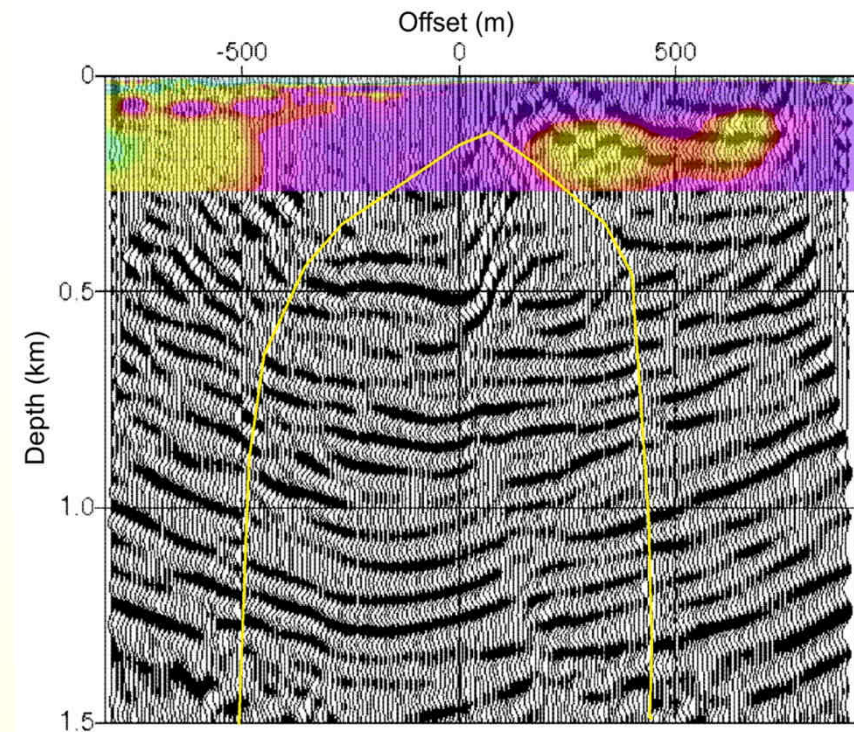
SWD RVSP migration

Interferometry
migration

Drill-bit seismic interferometry



Velocity model below the main SWD seismic line (velocity scale in m/s)



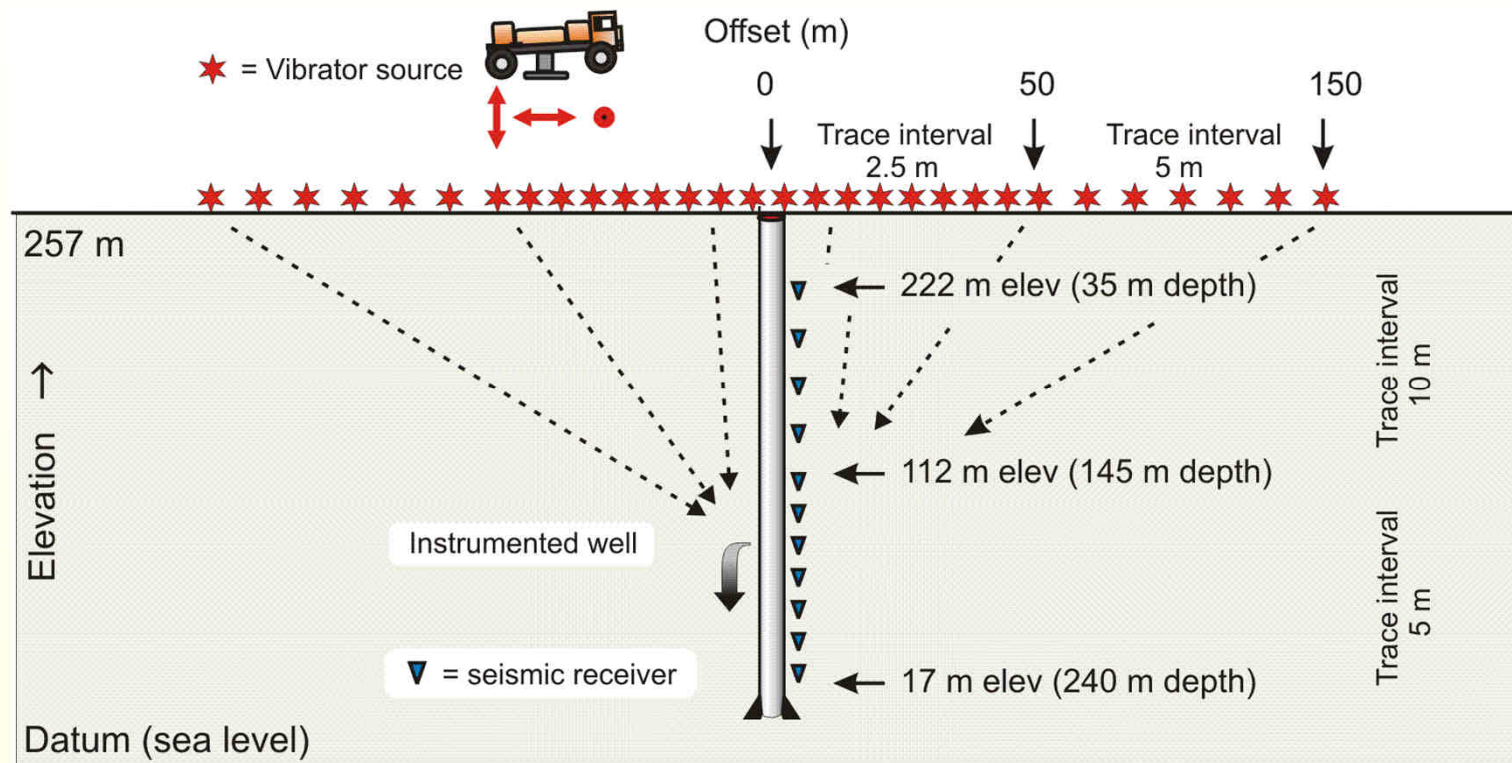
Combination of RVSP SWD migration and SWD interferometry migration, with magneto-telluric results on the top

Applications: example 3

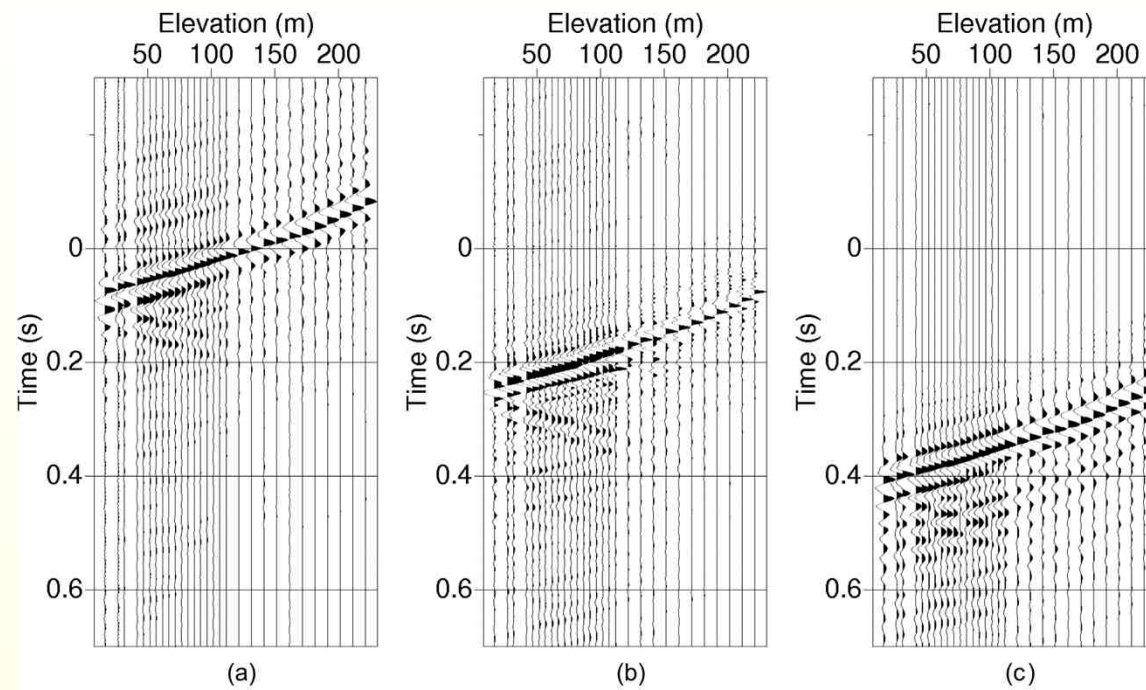


- ☐ Seismic interferometry experiment using single-well data recorded in a shallow well
- ☐ Surface vibrator source
- ☐ Improve vibrator signal by deconvolution

Experiment layout



Virtual and VSP signals



SI by correlation



❑ Using crosscorrelated vibrator signals

$$X_{Ai}(\omega) \propto G_{Ai}(\omega)V_i(\omega)$$

$$S_{Ai}(\omega) = X_{Ai}(\omega)P_i^*(\omega)$$

$$C_{AB}(\omega) = \sum_i X_{Ai}(\omega)X_{Bi}^*(\omega)P_i(\omega)P_i^*(\omega)$$

$$C_{AB}(\omega) \approx \sum_i G_{Ai}(\omega)G_{Bi}^*(\omega)V_i(\omega)V_i^*(\omega)P_i(\omega)P_i^*(\omega)$$

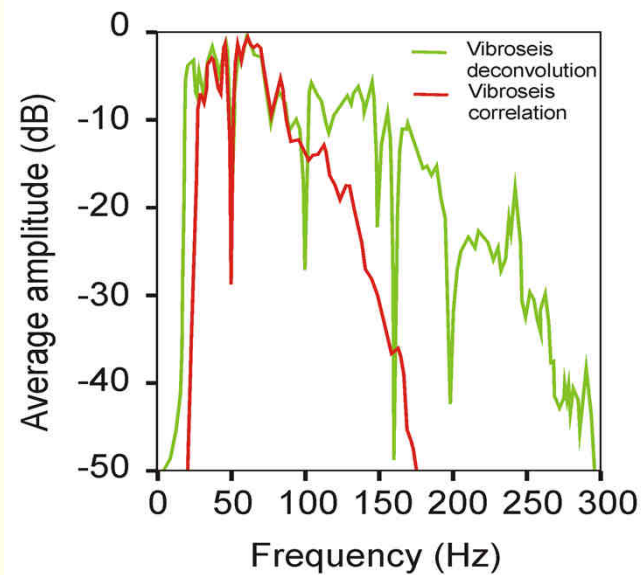
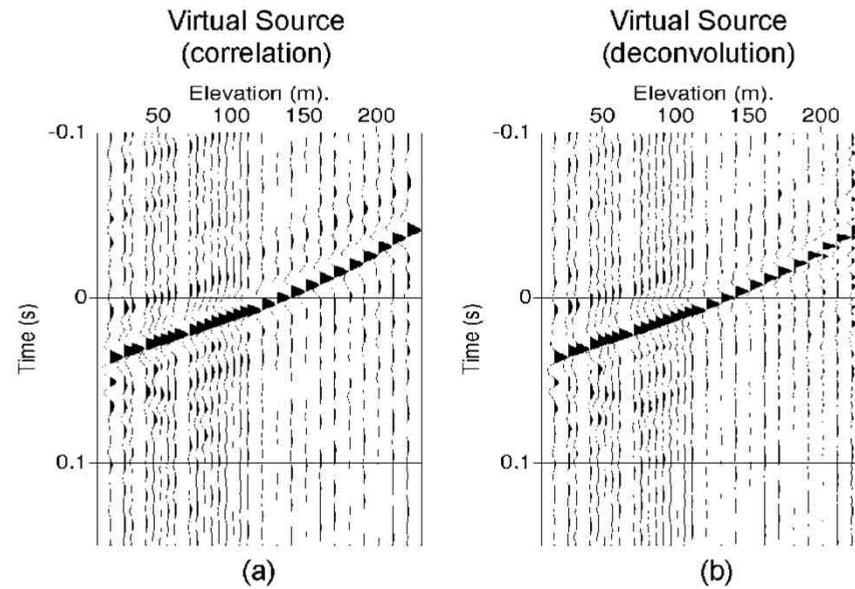
❑ Using deconvolved vibrator signals

$$S_{Ai}^D(\omega) = \frac{X_{Ai}(\omega)}{P_i(\omega)}$$

$$C_{AB}^D(\omega) = \sum_i S_{Ai}^D(\omega)(S_{Bi}^D(\omega))^* = \sum_i \frac{X_{Ai}(\omega)X_{Bi}^*(\omega)}{P_i(\omega)P_i^*(\omega)}$$

$$C_{AB}^D(\omega) \approx \sum_i G_{Ai}(\omega)G_{Bi}^*(\omega)\frac{V_i(\omega)V_i^*(\omega)}{P_i(\omega)P_i^*(\omega)}$$

Applications: example 3



Multidimensional approach to SI



- ❑ Use multidimensional SI deconvolution (MDD)
- ❑ Retrieve the Green's function removing the blurring effects of seismic interferometry

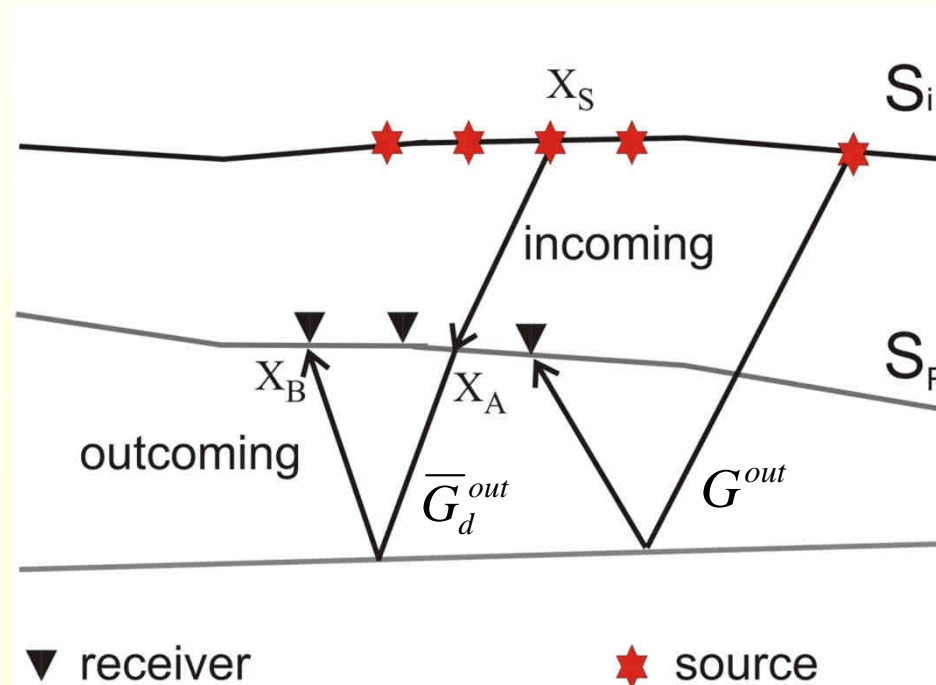
Seismic interferometry (SI) MDD



Using the Green's function by crossconvolution integral representation over the receiver surface S_R (Wapenaar, 2011; Wapenaar and van der Neut, 2010a) gives

$$G^{out}(x_B, x_S^{(i)}, t) * s^{(i)}(t) = s^{(i)}(t) * \int_{S_R} \overline{G}_d^{out}(x_B, x, t) * G^{in}(x, x_S^{(i)}, t) dx,$$

where "*" denotes time convolution. The approach needs separated wavefields at receivers (Metha et al., 2007; Wapenaar et al., 2010b).



SI point-spread function (PSF)



Crosscorrelating equation (1) by the incoming wavefield $u^{in}(x_A, x_S^{(i)}, t)$, using $u(t) \approx G(t) * s(t)$, and taking the sum over the source space S_i gives the normal equation

$$C(x_B, x_A, t) = \int_{S_R} \overline{G_d^{out}}(x_B, x, t) * \Gamma(x, x_A, t) dx, \quad (2)$$

where $C(x_B, x_A, t)$ is the virtual-source crosscorrelation function obtained using the incoming wavefield u^{in} and the outcoming wavefield u^{out} , and

$$\Gamma(x, x_A, t) = \sum_i u^{in}(x, x_S^{(i)}, t) * u^{in}(x_A, x_S^{(i)}, -t) \quad (3)$$

is the point-spread function (PSF) of seismic interferometry. Equation (2) is inverted for MDD purposes to get the outcoming Green's function $\overline{G_d^{out}}$.

Virtual reflector (VR) by convolution



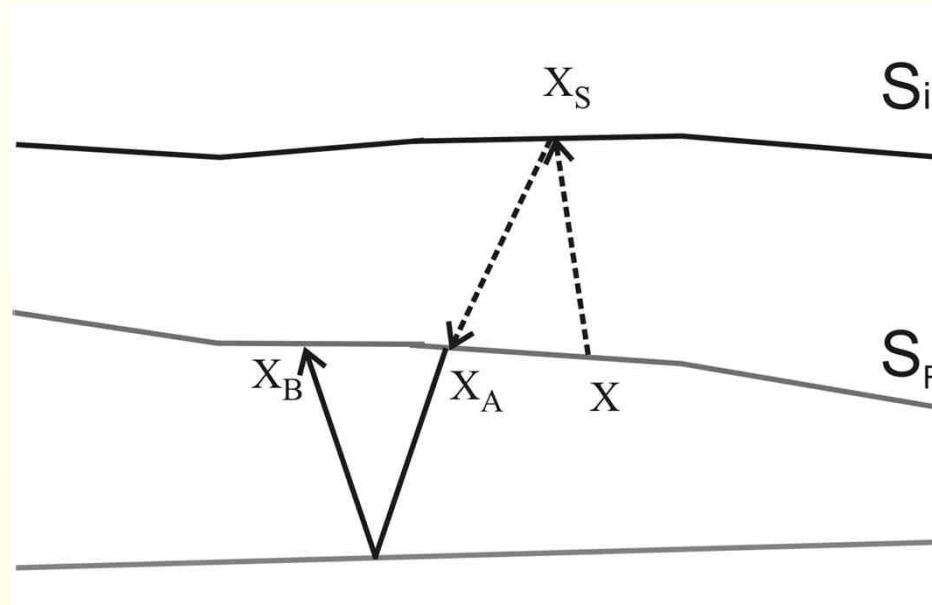
Starting from Eq. (1) we extend the approach using a modified representation by crossconvolution (Poletto and Farina, 2010), and we get

$$VR^{out}(x_B, x_A, t) = \int_{S_R} \overline{G}_d^{out}(x_B, x, t) * \Lambda(x, x_A, t) dx, \quad (4)$$

where

$$VR^{out}(x_B, x_A, t) = \sum_i u^{out}(x_B, x_S^{(i)}, t) * u^{in}(x_A, x_S^{(i)}, t) \quad (5)$$

is the outcoming virtual reflector (VR) interferometry function,



Virtual-reflector (VR) PSF

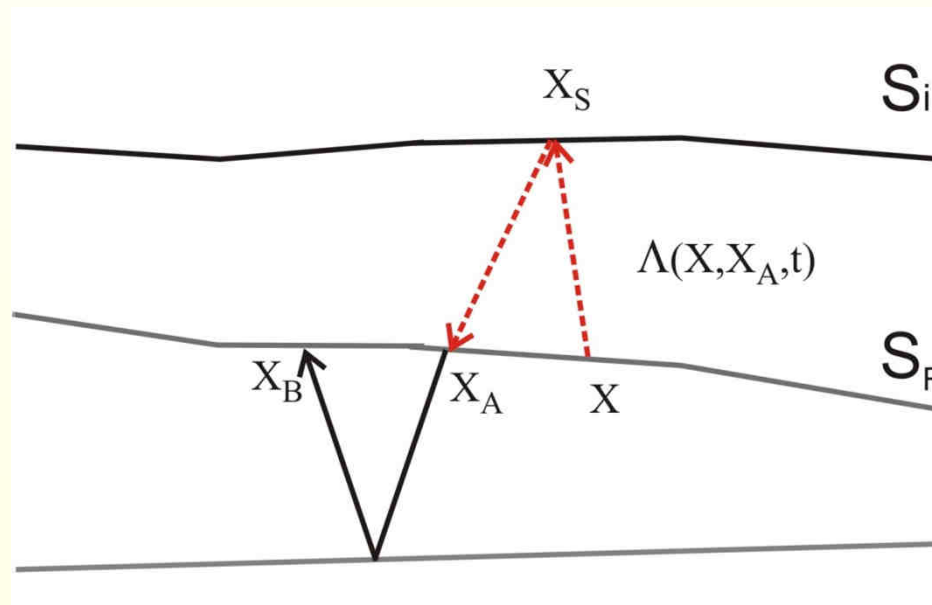


where

$$\Lambda(x, x_A, t) = \sum_i u^{in}(x, x_S^{(i)}, t) * u^{in}(x_A, x_S^{(i)}, t) \quad (6)$$

is the virtual reflector interferometry point-spread function (PSF).

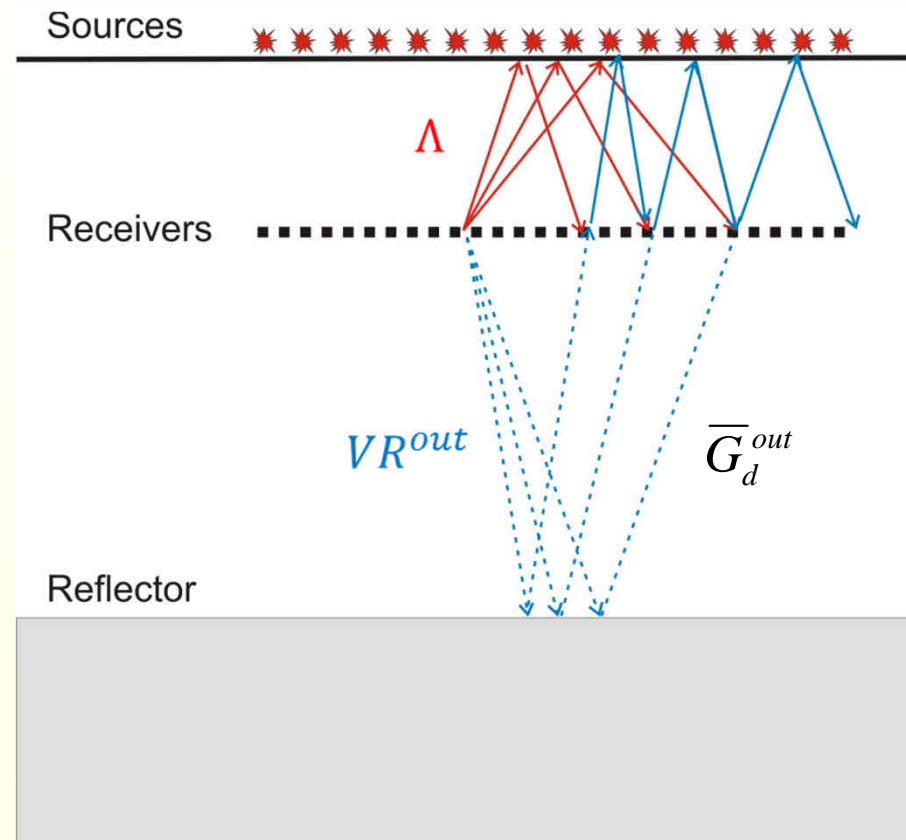
Note that Λ is a symmetric function, i.e., $\Lambda(x, x_A, t) = \Lambda(x_A, x, t)$.



VR multidimensional convolution



$$VR^{out}(x_B, x_A, t) = \int_{S_R} \overline{G}_d^{out}(x_B, x, t) * \Lambda(x, x_A, t) dx,$$



VR multidimensional deconvolution (MDD)



Inverting MD VR equation we obtain an estimate of the Green's function

$$\overline{G}_d^{out}(x_B, x, t) = \int_{S_R} VR^{out}(x_B, x', t) * \Lambda^{inv}(x', x, t) dx'. \quad (7)$$

The inverse PSF function Λ^{inv} satisfies the condition

$$\int_{S_R} \Lambda(x', \eta, t) * \Lambda^{inv}(\eta, x, t) d\eta = \delta(x' - x) \delta(t). \quad (8)$$